International Journal of Energy Research

INTERNATIONAL JOURNAL OF ENERGY RESEARCH
Int. J. Energy Res. (2014)
Published online in Wiley Online Library (wileyonlinelibrary.com). DOI: 10.1002/er.3163

REVIEW PAPER

An overview of unsolved deficiencies of direct methanol fuel cell technology: factors and parameters affecting its widespread use

Piyush Kumar, Kingshuk Dutta, Suparna Das and Patit Paban Kundu*,†

Advanced Polymer Laboratory, Department of Polymer Science and Technology, University of Calcutta, 92, A. P. C. Road, Kolkata 700009, India

SUMMARY

Direct methanol fuel cells (DMFCs) have evolved over the years as a potential candidate for application as a power source in portable electronic devices and in transportation sectors. They have certain associated advantages, including high energy and power densities, ease of fuel storage and handling, ability to be fabricated with small size, minimum emission of pollutants, low cost, ready availability of fuel and solubility of fuel in aqueous electrolytes. However, in spite of several years of active research involved in the development of DMFC technology, their chemical-to-electrical energy conversion efficiencies are still lower compared with other alternative power sources traditionally used. This review paper will focus on the existing issues associated with DMFC technology and will also suggest on the possible developmental necessities required for this technology to realize its practical potentials. Copyright © 2014 John Wiley & Sons, Ltd.

KEY WORDS

electrode kinetics; methanol crossover; electrode flow rate; membrane thickness; polarization; energy conversion efficiency

Correspondence

*Patit Paban Kundu, Department of Polymer Science and Technology, University College of Science and Technology, University of Calcutta, Kolkata 700009, India.
†E-mail: ppk923@yahoo.com

Received 8 February 2013; Revised 16 December 2013; Accepted 23 December 2013

1. INTRODUCTION

It was as early as in 1839 that William R. Grove discovered the basic operating principle of fuel cell technology by reversing water (H_2O) electrolysis to generate electricity from hydrogen and oxygen (O_2) [1]. This technology has attracted increased attention during the last couple of decades from both scientists and technologists all over the world [2–10]. A fuel cell is defined as an electrochemical energy conversion device that combines a fuel (hydrogen, natural gas, methanol (CH_3OH), gasoline, etc.) and an oxidant (air or O_2) and converts a fraction of their chemical energy into useful electrical power. Unlike a battery, a fuel cell does not store energy; it works in a continuous manner whenever fuel is delivered and is devoid of charge–discharge cycles. Thermodynamically, the most striking difference between a thermal engine and a fuel cell is that the former is limited by the Carnot efficiency, while the latter is not. Hence, fuel cells offer a quantum jump in terms of energy conversion efficiency and require no emission control systems as are necessary in conventional energy conversion devices [11,12]. Moreover, fuel cells practically avoid the emission of toxic gases, such as sulfur dioxide and nitrogen oxides (NO_x) [13,14]. In the present scenario, when protecting global environment has become a serious issue [15], development of fuel cells has gained more acceptance as a highly promising technology to solve problems associated with energy resources, atmospheric pollution, green house effects and global warming, because they provide high efficiency and low emissions.

Fuel cell systems can be classified on the basis of various parameters, which include the nature and type of fuel used, whether the fuel is processed externally (external reforming) or internally (internal reforming), operating temperature, operating pressure and type of electrolyte used. However, for practical reasons, they are simply distinguished by the type of electrolyte used. The six generic fuel cells in various stages of development are as follows: (i) proton exchange membrane fuel cells [16]; (ii) direct CH_3OH fuel cells (DMFCs); (iii) alkaline fuel cells; (iv) phosphoric acid fuel cells; (v) molten carbonate fuel cells; and (vi) solid oxide fuel cells. Among these, the polymer electrolyte hydrogen/air fuel cells and DMFCs

are the most promising systems for providing power to portable devices and in transportation sectors [17,18].

Although hydrogen has proven to be the best fuel in terms of energy conversion (chemical to electrical) efficiency, its production, storage and distribution have several associated problems [19,20]. Compared with hydrogen, CH_3OH as a liquid fuel offers many advantages, such as higher energy density (6100 $Wh\,kg^{-1}$ at 25 °C), being relatively cheaper, ease of storage and handling, ready availability and solubility in aqueous electrolytes [21,22]. Because it can be readily derived from oil, natural gas, coal or biomass, there is ample scope for its availability as a fuel. As a liquid under normal conditions, CH_3OH can be easily dispensed within the current fuel network. In addition, CH_3OH needs no cryogenic storage container. CH_3OH can be completely electro-oxidized to carbon dioxide (CO_2) at temperatures well below 100 °C at a fuel cell anode, either directly or indirectly. If used indirectly, CH_3OH needs to be initially reformed to give hydrogen via a high-temperature step. Thus, CH_3OH can be used directly in DMFCs, or indirectly as a hydrogen source for polymer electrolyte membrane (PEM) fuel cells after reformation. However, the latter approach includes extensive and multistep purification of the fuel, after which the resulting hydrogen-rich mixture can be supplied to the proton exchange membrane fuel cell; therefore, this approach is associated with several engineering complexities, as well as considerably lower power delivery after extended applications [23]. In totality, the DMFC technology provides the following advantages: (i) elimination of the need for fuel storage; (ii) high energy density of the fuel; and (iii) modular, vibration-free and silent operation. Moreover, because CH_3OH is fed directly as a diluted aqueous solution, it also avoids complex humidification and thermal management problems associated with hydrogen fuel cells. These advantages led researchers to conclude that DMFC operating at low/medium temperatures of up to 130 °C is the most favorable option for mobile and portable applications.

As a device, proper working of DMFC demands optimum and cooperative functioning of its various constituent parts. Although many review articles are available on the subject of 'DMFCs', however, most of them provide in-depth discussion on individual specialized constituent parts, rather than the overall device. Because we in our lab aim at analyzing and optimizing the participation of each constituent in order to realize a better overall DMFC performance [6,8], therefore, we thought it necessary to present this review article, which will provide an overall view of the DMFC device, the restricting factors delaying its commercialization prospects and essentially the possible ways out that can eventually establish this highly prospective device as a true alternative to conventional energy sources as well as other established alternative energy-harnessing devices.

2. BASICS OF DIRECT METHANOL FUEL CELL TECHNOLOGY

2.1. Working principle

Direct methanol fuel cell uses CH_3OH in the form of vapor or liquid as fuel and consists of a solid polymer electrolyte. A schematic illustration of a DMFC has been shown in Figure 1. It consists of an anode at which CH_3OH gets electro-oxidized to CO_2, represented by the reaction

$$CH_3OH + H_2O \rightarrow CO_2 + 6H^+ + 6e^- \quad (E^\circ = 0.02\ V/SHE) \tag{1}$$

where SHE stands for standard hydrogen electrode and a cathode at which O_2 (usually air) gets reduced to form H_2O or steam by the reaction

$$3/2O_2 + 6H^+ + 6e^- \rightarrow 3H_2O \quad (E^\circ = 1.229\ V/SHE) \tag{2}$$

Accordingly, the net cell reaction in a DMFC can be given as

$$CH_3OH + 3/2O_2 \rightarrow CO_2 + 2H_2O \quad (E_{cell} = 1.213\ V) \tag{3}$$

The basic operating principle of a DMFC system can be realized with the help of a PEM fuel cell model shown in Figure 2 [24]. CH_3OH flows through the anode flow channel, diffuses through the anode diffusion layer and reaches the anode catalyst layer where it is catalytically oxidized, resulting in the release of electrons and protons as detailed in Reaction 1. The released electrons get conducted through the metal catalyst and carbon grains and arrive at the cathode side of the cell via the external circuit. On the other hand, protons get transported through the PEM to the cathode catalyst layer. Simultaneously, O_2 or air is fed into the cathode flow channel, where it diffuses through the diffusion layer and reaches the catalyst layer. Here, it reacts with the generated protons and electrons to produce H_2O according to Reaction 2. The Gibbs free energy of CH_3OH and O_2 is much higher than those of H_2O and CO_2. Consequently, the combustion of CH_3OH is a spontaneous reaction under standard conditions of 298.15 K temperature and 1 atm pressure. This energy difference facilitates the production of electrical energy.

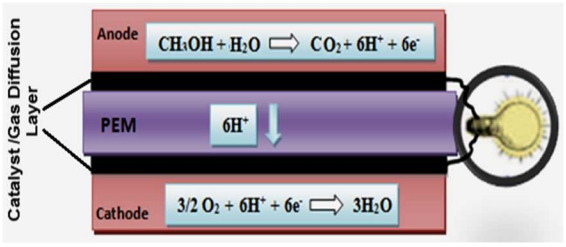

Figure 1. A schematic illustration of a direct methanol fuel cell.

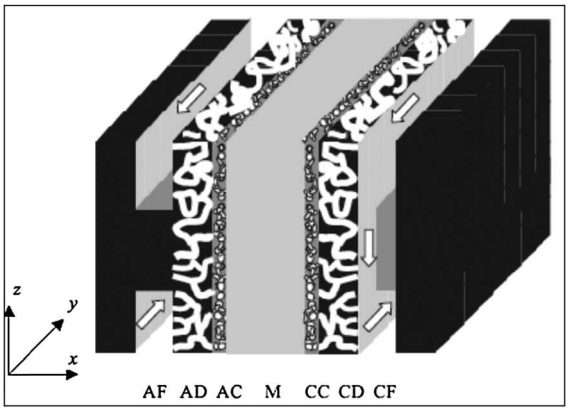

Figure 2. A three-dimensional schematic representation of a polymer electrolyte membrane fuel cell. AF, anode flow channel; AD, anode diffusion layer; AC, anode catalyst layer; M, polymer electrolyte membrane; CC, cathode catalyst layer; cathode (CD), diffusion layer; CF, cathode flow channel. Reproduced with permission from [24], copyright © 2004 WILEY-VCH Verlag GmbH & Co. KGaA, Weinheim.

A CH_3OH-feed fuel cell has several advantages over the cells designed for gaseous fuel-feed systems. These are the following: (i) elimination of the fuel vaporizer and its associated heat source and controls; (ii) elimination of complex humidification and thermal management systems; (iii) dual-purpose use of the liquid CH_3OH/H_2O as fuel and as an efficient stack coolant; and (iv) significantly lower size, weight and temperature of the system.

2.2. Components and their functions

Typically, a DMFC is composed of a membrane electrode assembly (MEA), bipolar plates, gaskets, current collector and end plates. The different components and their functions have been presented in Table I.

2.2.1. Membrane electrode assembly

The MEA is often considered as the heart of a DMFC and consists of a proton exchange membrane, catalyst layers and gas diffusion layers (GDLs) (Figure 3). Usually, these components are fabricated individually and then pressed together at high temperatures and pressures [8,25,26]. However, this technique suffers from the drawback that Nafion® (Du Pont de Nemours, USA) that gets impregnated into the active layer of the electrode has a limited penetration depth, which in turn reduces the electrochemically active area between the electrocatalyst particles and the ionomer, resulting in decreased catalyst utilization [27]. Jung *et al*. [28] tried to overcome this particular problem by annealing the MEA at various temperatures, that is, at 110, 130, 150 and 200 °C. They found that annealing at 130 °C, which is near the glass transition temperature of the recast Nafion binder, can result in the binder exhibiting the highest proton conductivity. The polarization curves of the cells based on MEA annealed at different temperatures have been presented in Figure 4a. Tang *et al*. [29] investigated the difference of performance rendered by varying the fabrication methods. By utilizing a conventional hot-pressed MEA and catalyst-coated membrane (CCM), they found that compared with the hot-pressed MEA, the cell with CCM exhibited a decreased CH_3OH crossover by 55% along with an increased power density by 36% (Figure 4b). This enhanced performance exhibited by CCM was found to be a result of the significantly higher electrochemical reaction areas and improved catalyst/membrane interface, resulting in reducing the loss of Pt electrocatalysts to the GDLs. Krishnan *et al*. [30] developed a modified form of low-temperature decal (LTD) method for fabricating MEAs that use hydrocarbon (HC)-based membranes for DMFCs. The MEAs (with HC-based membranes) fabricated by the modified LTD method were found to maintain good interfacial contact between the catalyst layers and the membranes, which led to decreased contact resistances and increased performances of the cell by more than 20% when compared with that obtained for the MEAs fabricated by following the conventional LTD method (Figure 5).

The electrode catalyst layers are referred to as the active layers in the DMFC operation, as they are the locations of the half-cell reactions (Reactions 1 and 2). The catalyst layers have a film-like structure and consist of the following materials: (i) carbon black particles (usually Vulcan XC-72) as electrical conductor and catalyst support (if the catalyst is used as supported); (ii) poly (tetrafluoroethylene) (PTFE) as hydrophobic element that also provides mechanical stability by holding the carbon particles; and (iii) an ionomer (usually Nafion) to promote the proton transport and confine the electrodes and the polymer electrolyte [31,32]. Generally, a binary catalyst Pt/Ru is applied at the anode, while only Pt is used as catalyst at the cathode. Catalyst loadings between 1 and 5 mg cm^{-2} are normally applied for DMFC operation [33]. However, because Pt is a very expensive material, high Pt loadings cause a major barrier to the commercialization of DMFCs. For effective operation, it is important that the catalyst should have a high active surface area, minimized poisoning from CO and high dispersion [34].

On the other hand, GDLs facilitate the transport of CH_3OH and O_2 to the anode and cathode catalyst layers, respectively. In addition, GDL also allows the conduction of electrical current out of the cell and provides the MEA with mechanical stability by holding the porous film-like catalyst structure [35]. The most required criteria of a GDL material are that it must be porous and conductive. The porous carbon paper or carbon cloth, with a thickness in the range of 100–300 μm is mostly used to allow the transport of reactants, as well as products [35], that is, CO_2 and H_2O, at the anode and the cathode, respectively, in order to prevent the blockage of the transport paths in the electrodes. Usually, the diffusion layers are coated with PTFE to increase the hydrophobicity, which in turn prevents the flooding of carbon cloth channels and promotes gas transport [32]. A very recent investigation on the effect of PTFE content on the performance of a DMFC has been reported by

Table I. The different components of a DMFC and their functions.

DMFC components		Functions/roles	Preferably used	References
MEA	Polymeric membrane	To exchange proton To repulse the electron	Nafion 117, 115, 112	[26,31–33]
	Catalyst layer (anode)	Proton conduction Electron conduction Catalysis (oxidation at anode) Transportation of water Heat management within cell compartment	Pt/Ru/C	[8,26,34,68]
	Catalyst layer (cathode)	Proton conduction Electron conduction Catalysis (reduction at cathode) Oxygen transport Water management Heat management within cell compartment	Pt/C	[8,34,68]
	Gas diffusion layer	To move outward the generated gas (CO_2) from the surface of PEM	Vulcan XC-72 (carbon paper/cloth)	35
Bipolar plate	Anode side	To distribute the fuel at MEA Electron conduction Heat transfer	Nonporous graphite Coated metals Composite material	[43–46]
	Cathode side	To distribute the oxidant at MEA Electron conduction Heat transfer	Nonporous graphite Coated metals Composite material	[43–46]
Gaskets	Anode side	Preventing of fuel leakage	Silicon rubber Teflon sheet	[51]
	Cathode side	Preventing of oxidant leakage	Silicon rubber Teflon sheet	[51]
Current collector plate	Anode side	To collect the generated current To conduct the collected current	Copper Gold-plated copper Stainless steel Gold-plated nickel	[52]
	Cathode side	To conduct the current from the outer circuit to the reactant	Copper Gold-plated copper Stainless steel Gold-plated nickel	[52]
End plates	Anode side	To provide the compactness of a cell system	SS plate	[53]
	Cathode side	To provide the compactness of a cell system	SS plate	[53]

DMFC, direct methanol fuel cell; MEA, membrane electrode assembly; PEM, polymer electrolyte membrane.

Krishnamurthy and Deepalochani [36]. They found a 15% PTFE content to be optimum for anode GDL and 20% for anode microporous layer (MPL), whereas a 20% PTFE content was found to be optimum for both cathode GDL and MPL (Figure 6). It is also very crucial to control the structure of the GDL for effecting appropriate mass transport in a DMFC [37]. Accordingly, many works have focused on the functional characteristics of the GDL, such as morphology, porosity, gas permeability and wettability [38,39]. For example, Park *et al.* [40] reported that MEAs using MPL-modified cathode GDLs (GDL-1) exhibit slightly better performance (117 mW cm^{-2}) at 0.4 V and 70 °C than commercial GDL-based (SIGRACET product version: GDL-35BC, SGL Co., SGL Group – The Carbon Company). MEAs (110 mW cm^{-2}) (Figure 7).

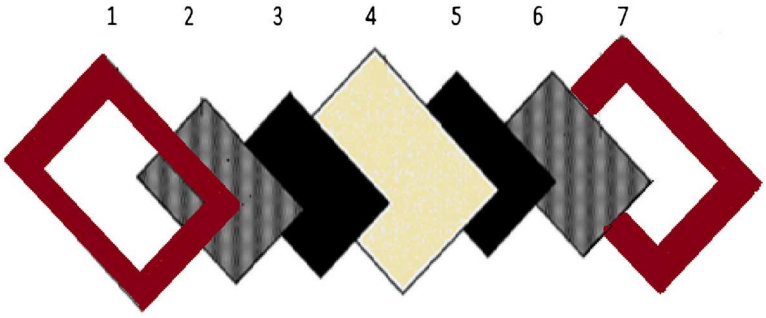

Figure 3. Constituent parts of a membrane electrode assembly: gasket seal (1 and 7), gas diffusion layers (2 and 6), catalyst layers (3 and 5) and polymer electrolyte membrane (4).

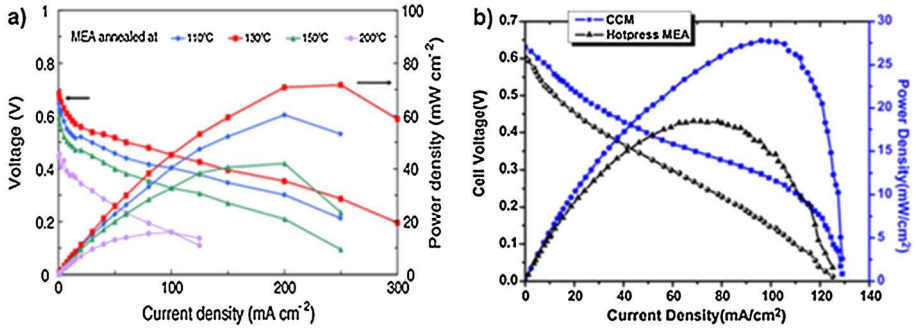

Figure 4. (a) The polarization curves of the cells based on membrane electrode assembly (MEA) annealed at different temperatures. Reprinted from [28], copyright © 2007, Elsevier. (b) Comparative analysis of the hot-pressed MEA with the catalyst-coated membrane (CCM) in terms of cell performance. Reprinted from [29], copyright © 2007, Elsevier.

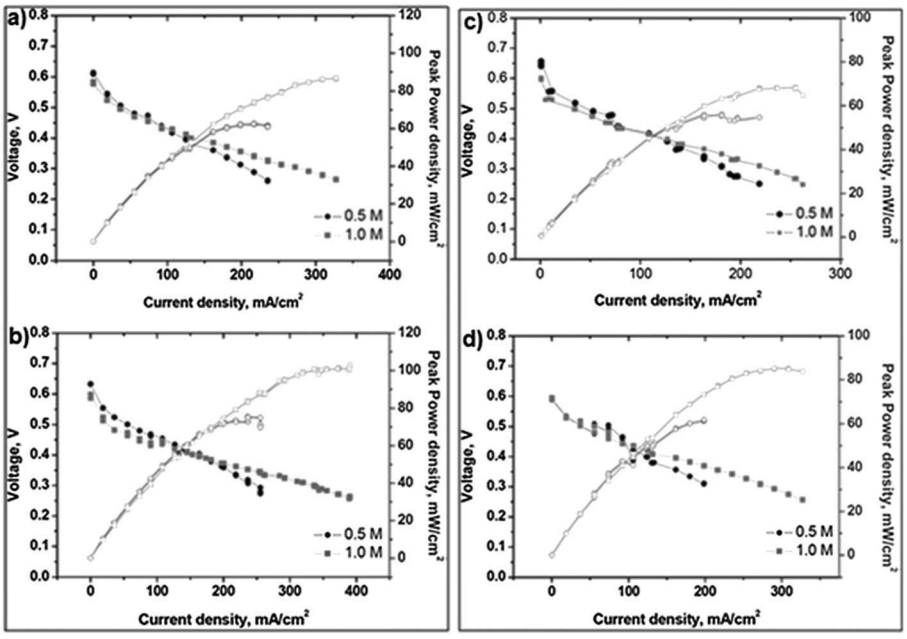

Figure 5. Direct methanol fuel cell performance of (a) a modified low-temperature decal (LTD) membrane electrode assembly (MEA) with a commercial hydrocarbon (HC) membrane and (b) a modified LTD MEA with a KRICT HC-based membrane; and (c) a conventional LTD MEA with a commercial HC membrane and (d) conventional LTD MEA with a Korea Research Institute of Chemical Technology (KRICT) membrane. Reprinted from [30]. Copyright © 2010 with permission from Professor T. Nejat Veziroglu and International Association for Hydrogen Energy.

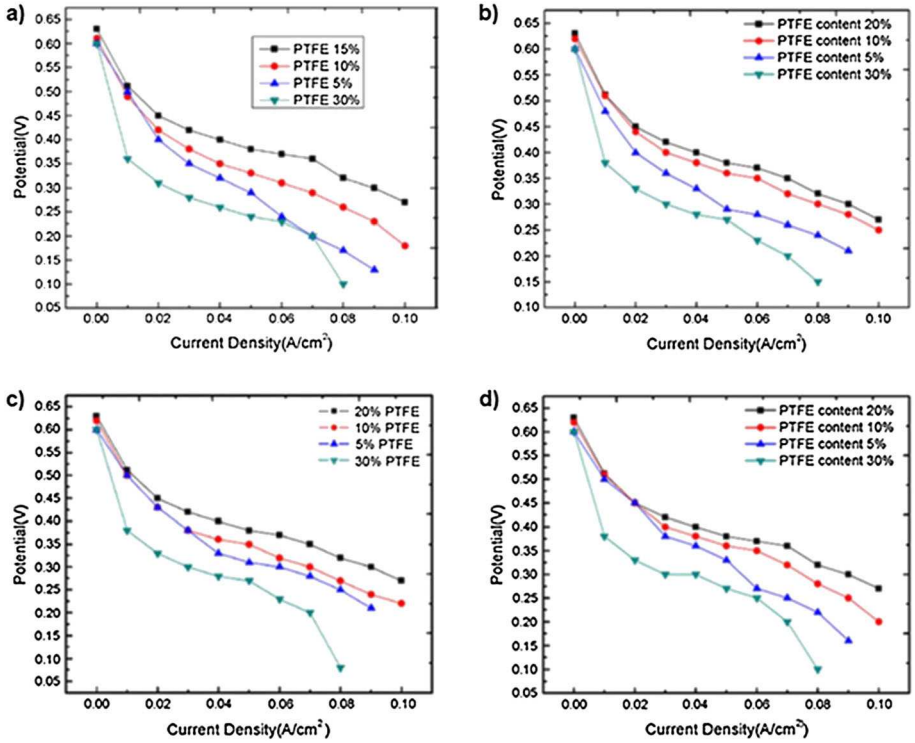

Figure 6. Effect of poly(tetrafluoroethylene) (PTFE) content on the performance of direct methanol fuel cell: (a) in the anode gas diffusion layer, (b) in the anode MPL, (c) in the cathode MPL and (d) in the cathode backing layer. Reprinted from [36]. Copyright © 2009 with permission from Professor T. Nejat Veziroglu and International Association for Hydrogen Energy.

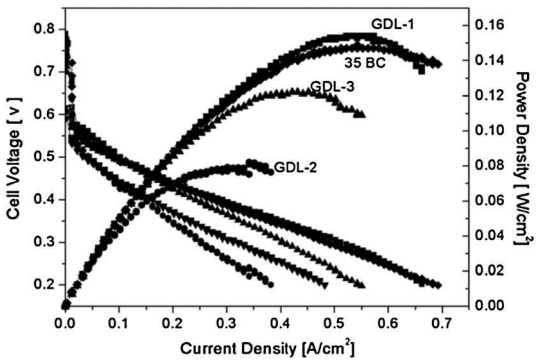

Figure 7. Direct methanol fuel cell performances of membrane electrode assemblies at 0.4 V, using different cathode gas diffusion layers (GDLs) at an operating temperature of 70 °C. Reprinted from [40]. Copyright © 2009 with permission from Professor T. Nejat Veziroglu and International Association for Hydrogen Energy.

2.2.2. Bipolar plates

Bipolar plates are generally used to distribute the fuel and the oxidant within the cell and separate the individual cells in the stack. They also contribute in collecting and distributing current, humidifying gases and keeping the cells cool. Plate topologies and materials facilitate these functions. Flow-field designs, including flow-field profiles, depths, widths and lengths, have a major impact on the overall performance of DMFC [8,41]. The plate topologies may include straight, serpentine or interdigitated flow fields, internal manifolding, internal humidification and integrated cooling. For effective operation, the major criteria are that the bipolar plates should have a good conductivity, mechanical strength and ability to handle acid–base conditions [42]. Materials are chosen on the basis of chemical compatibility, resistance to corrosion, cost, gas diffusivity, material strength and thermal conductivity. From the points of weight, volume and cost, the bipolar plate has much importance in a cell system. The commonly used materials for bipolar plates include nonporous graphite, a variety of coated metals and a number of composite materials [43–46]. Mehta *et al.* [47] reviewed the various designs and fabrication techniques regarding the bipolar plates. A comparative analysis regarding the advantages and disadvantages experienced using graphite, coated metal and composite bipolar plates has been listed in Table II. Recently, Reza *et al.* [48] developed a nanocomposite bipolar plate, consisting of 40 wt% phenolic resin as binder and 45 wt% graphite, 10 wt% nanosheet expanded graphite and 5 wt% carbon fiber as fillers. Using this modification, the authors achieved a maximum power density as high as 812 mW cm^{-2} and a current density of 900 mA cm^{-2} at 0.6 V, which are better than the cells prepared by using metallic and commercial bipolar plates.

2.2.3. Gasket, current collector and end plates

In a DMFC system, a gasket prevents leaking of reactants and isolates current between the current collector and end

Table II. A comparative analysis regarding the advantages and disadvantages experienced using graphite, coated metal and composite bipolar plates.

Component	Types	Advantages	Disadvantages
Bipolar plate	Nonporous graphite	High corrosion resistance	Poor machining
		Thermal conductivity	Expensive
		High gas permeability	Poor compressive strength
		Excellent electrical conductivity	
	Coated metal	High compressive strength	Susceptibility to corrosion
		Much higher conductivity of heat and electricity	High cost
		Very easy machining (e.g., stamping)	Lower chemical resistance
		High modulus	
	Composite	Low cost	Lower conductivity
		High availability	Less mechanical strength than metal plates
		High chemical resistance	
		Gas impermeability	

plates. Usually, silicon rubber is used as the gasket material. It is very important to maintain the thickness of the gasket when the MEA gets sandwiched between the bipolar plates, as it potentially affects the cell performance by influencing the internal resistance. For example, a thicker gasket can increase the overall thickness of the MEA, which in turn increases the total internal resistance [49]. In addition, carbon paper is a fragile commodity and is therefore prone to be crushed by the collector ribs under conditions when the gasket thickness gets unmatched or the compressing pressure becomes too high. Table III tabulates the appropriate thickness of the gasket corresponding to the respective carbon paper thickness [50].

The current collector carry current generated in the MEA, and end plates maintain the compactness of the system. Copper, gold-plated copper, stainless steel, gold-plated nickel and so on are used for the fabrication of the current collector [51,52]. On the other hand, materials that are mechanically strong and electrically nonconductive are used for making the end plates [53].

3. LIMITING FACTORS OF DMFC

The thermodynamically reversible cell potential for the overall DMFC reaction is 1.21 V (Reaction 3). This is comparable with the corresponding value of 1.23 V for the hydrogen fuel cell. Nevertheless, the DMFC technology has a number of drawbacks in terms of performance and efficiency. The major deficiencies that are still hindering its widespread commercialization can be summarized as follows: (i) sluggish kinetics of CH_3OH oxidation and oxygen reduction reaction (ORR) at the cell anode and cathode, respectively. The slow anode reaction near the thermodynamic potential for the catalysts that are currently used constitutes a significant fraction of the overall voltage loss. On the other hand, the overpotential of ORR at the cell cathode has been reported to be over 200 mV under open-circuit condition, even on the most active Pt surface [54,55]. Moreover, a chemical short circuit, resulting from CH_3OH crossover from the anode side to the cathode side of the cell, leads to an extra potential loss of more than 100 mV [56]. This effectively means that the efficiency loss occurring only at the cell cathode constitutes about 25% efficiency reduction from the theoretically calculated cell efficiency value [11,57,58]; (ii) DMFC performance suffers seriously from the CH_3OH crossover phenomenon occurring through the PEM (this crossover dramatically lowers the cell voltage, especially close to open-circuit conditions and also reduces the Faradaic efficiency of the cell); (iii) CH_3OH oxidation is accompanied by the release of a large amount of gaseous CO_2, which disturbs the flow in the anode flow field and hinders CH_3OH transport to the catalyst sites; and (iv) the high flux of liquid H_2O through the membrane retards O_2 transport to the catalyst sites, thereby increasing the voltage loss on the cathode side of the cell.

Table III. Thickness of gasket corresponding to thickness of C paper.

Types of carbon paper	Thickness of carbon paper (mm)	Thickness of gasket (mm)
Toray carbon paper-030	0.09	0.11
Toray carbon paper-060	0.17	0.17
Toray carbon paper-090	0.26	0.26
Toray carbon paper-120	0.35	0.33

Reprinted from [50]. © 2006 Elsevier Ltd.

These performance-lowering factors have warranted the necessity to overcome the following four key technical challenges: (i) low rate of CH_3OH oxidation kinetics at the anode and ORR at the cathode; (ii) CH_3OH crossover through the polymeric membrane; (iii) H_2O management on the cathode side of the cell, which is associated with the flow-field and backing designs; and (iv) gas management at the anode. These critical factors are described in detail later and have been tabulated in Table IV.

3.1. Electrode kinetic limitations

In principle, it follows from Reaction 1 that CH_3OH should get oxidized spontaneously when the potential of the anode

Table IV. Different limitations of DMFCs, their causes and the approaches for solving these problems.

Limitations of DMFC	Reasons	Target area	Approaches	References
Sluggish kinetics of methanol oxidation	Blocking of active platinum site by generated CO (poisoning effect)	Anode catalyst Particle size of catalyst material	Use of binary or multimetallic Pt alloys with metals, such as Sn, Ru, Os, Mo, Ir, W and so on	[67–80,97,98]
	Lower catalyst surface area		Use of high surface area of catalyst materials (nano-sized/micro-sized)	[78–83,96,97]
			Use of oxide structure with Pt	[81]
			Use of new catalyst system	[86,89,90]
Methanol crossover	Diffusion Electro-osmotic drag across the membrane	Operating parameters	Cell temperature, fuel concentration, flow rate and so on	[123–130,132–134]
		Anode catalyst	Use of highly active catalyst	[98,128]
		PEM	Use of hydrophobic materials	[140–144]
Water management at cathode (cathode flooding)	Electro-osmotic drag of water from the aqueous anode to cathode	MEA Flow rate	Use of more hydrophobic material at cathode backing layer	[125,86,151–160]
	Reduction reaction of O_2/air at cathode	Humidification of air/O_2	Use of least humidified oxidant	[86,127,153]
		Cathode pressure	Use high cathode pressure	
Gas management at anode (removal of CO_2)	Electro-oxidation of methanol	Flow channel design	Use of serpentine channel Two-phase flow pattern	[154,130,151,152]
		Gas diffusion layer	Use of highly porous and more hydrophilic material at anode backing layer	[86,125]

DMFC, direct methanol fuel cell; MEA, membrane electrode assembly; PEM, polymer electrolyte membrane.

Int. J. Energy Res. (2014)
DOI: 10.1002/er

is above 0.02 V versus SHE, while from Reaction 2, it is realized that O_2 should be reduced spontaneously when the cathode potential falls below 1.23 V versus SHE. Hence, in effect, DMFC would produce a cell voltage of 1.21 V at 100% voltage efficiency (Reaction 3), and this is not dependent on current demand. Thus, although DMFC operations are theoretically guided by thermodynamically favorable reactions, in reality, both the anode and cathode reactions are kinetically limited owing to its irreversible nature. Figure 8 summarizes the key performance-limiting issues associated with the DMFC electrodes [59].

The polarization losses arising because of the slow kinetics occurring at the DMFC electrodes are comparable with that of the hydrogen fuel cells, where polarization losses primarily occur at the cathode. A number of works have been performed to analyze the anodic oxidation of CH_3OH [60–62], and these resulted in the postulations of its reaction mechanism [63–65]. The most accepted of these postulates follow a bifunctional mechanism [64,65], comprising of C–H bond activation (Reactions 4 and 5) and H_2O adsorption (Reaction 6). The important steps of this postulate are represented as follows:

CH_3OH adsorption:

$$Pt + CH_3OH \rightarrow Pt - (CH_3OH)_{ads.} \quad (4)$$

C–H bond activation:

$$Pt - (CH_3OH)_{ads.} \rightarrow Pt - (CH_3O)_{ads.} + H^+ + e^- \quad (5a)$$

$$Pt - (CH_3O)_{ads.} \rightarrow Pt - (CH_2O)_{ads.} + H^+ + e^- \quad (5b)$$

$$Pt - (CH_2O)_{ads.} \rightarrow Pt - (CHO)_{ads.} + H^+ + e^- \quad (5c)$$

$$Pt - (CHO)_{ads.} \rightarrow Pt - (CO)_{ads.} + H^+ + e^- \quad (5d)$$

H_2O adsorption:

$$M + H_2O \rightarrow M - (H_2O)_{ads.} \quad (6)$$

where M stands for Ru, Sn, Os, W and other elements or compounds able to produce H_2O displacement at low potentials.

CO oxidation:

$$Pt - (CO)_{ads.} + M - (H_2O)_{ads.} \rightarrow Pt + M + CO_2 + 2H^+ + 2e^- \quad (7)$$

Net reaction:

$$CH_3OH + H_2O \rightarrow CO_2 + 6H^+ + 6e^- \quad (8)$$

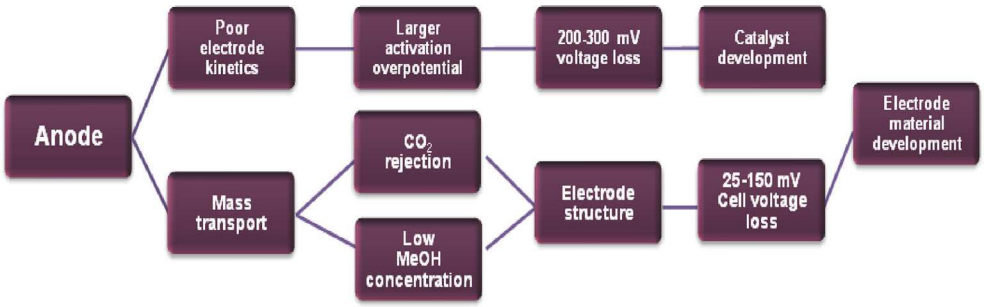

(a)

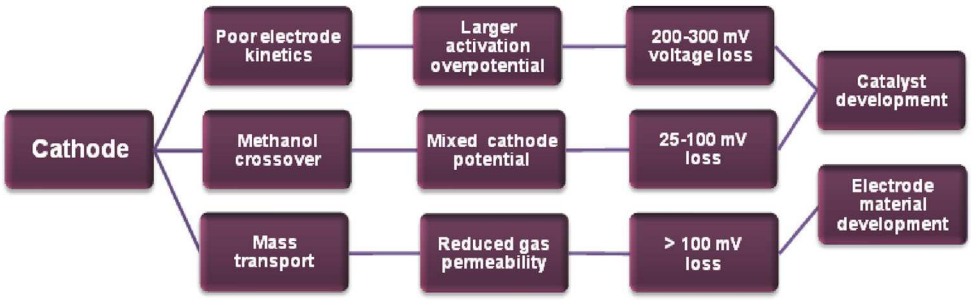

(b)

Figure 8. Technological limitations with (a) the direct methanol fuel cell (DMFC) anode and (b) the DMFC cathode. Reprinted from [59], copyright © 2010, with permission from Professor T. Nejat Veziroglu and International Association for Hydrogen Energy.

CH_3OH oxidation kinetics is sluggish because Pt–Ru does not adequately activate H_2O according to Reaction 6. On the other hand, the ORR can follow two different reaction pathways: (i) the direct four-electron pathway; and (ii) the peroxide pathway [66]. However, CH_3OH crossover from the anodic side to the cathodic side of the cell hampers O_2 reduction by blocking the Pt sites on the cathode. This is because CH_3OH after crossover reacts directly with O_2 at these sites, resulting in severe reduction of fuel efficiency. In addition, CH_3OH crossover reduces the cell voltage by generating a mixed potential and produces H_2O that causes cell flooding and increases the required O_2 stoichiometry.

The formation of adsorbed OH on the Pt surface, occurring in the H_2O adsorption step, is necessary for the oxidative removal of CO; however, this requires a high potential. In terms of anodic CH_3OH oxidation, such a high potential limits the application of a pure Pt catalyst. Therefore, the utility of a second metal that can act as a promoter by providing oxygenated species at lower potentials for oxidative removal of adsorbed CO has been investigated [67,68]. Subsequently, many binary and multimetallic Pt-based alloy compositions, such as Pt/Ru, Pt/Os, Pt/Sn, Pt/Mo, Pt/Ir, Pt/Ru/Sn/W and Pt/Ru/Sn, have been proposed for the purpose of improving the electro-oxidation of CH_3OH [67–77]. However, the use of Pt in combination with non-noble metals as an anodic catalyst material for CH_3OH electro-oxidation poses two major limitations: (i) uncertainty over long-term stability; and (ii) uncertainty and time dependence of the available active surface area due to a leaching out effect. Because of these limitations, recent years have seen increased interest in developing dispersed micrometal/nanometal particles supported on high-surface-area materials as catalysts [78–83]. These new catalyst systems present unique physical and chemical properties [84,85]. Mu *et al.* [78] developed a method to load Pt nanoparticles on carbon nanotubes (CNTs) without the requirement of pretreating the CNTs. They showed that the Pt/CNT composite modified by the organic molecule triphenylphosphine (PPh_3) has higher electrocatalytic activities and enhanced tolerance toward catalyst poisoning species than the commercial E-TEK catalyst. The PPh_3 has been reported to act as a crosslinker, which exhibits sufficient reduction in catalyst agglomeration during DMFC operation. Zhou *et al.* [81] prepared Pt/MnO_2/CNT and Pt–Ru/MnO_2/CNT nanocomposites by successively loading hydrous MnO_2 ($MnO_2{\cdot}xH_2O$) and Pt (or Pt/Ru alloy) nanoparticles on CNTs, to be used as anodic catalysts in DMFCs. Because of the presence of MnO_2 on the surface of CNTs, Pt/MnO_2/CNT showed a higher electrochemically active surface area (EASA) and better CH_3OH electro-oxidation activity, compared with Pt/CNTs. However, although MnO_2 in the Pt/MnO_2/CNT catalyst increased the EASA of Pt, it failed to enhance its CO oxidation ability. Replacing Pt by Pt/Ru alloy nanoparticles in the preparation of catalyst nanocomposites resulted in overcoming this problem. The Pt–Ru/MnO_2/CNT catalyst exhibited excellent electro-oxidation of CH_3OH, as well as good CO oxidation ability; and this is supported by the onset potential and peak potential values [81]. Xu *et al.* [82] extensively studied some important nanocatalyst systems, such as Pt/Ru nanocomposites, Au nanocatalysts and multiwalled CNT (MWNT)-supported Pt/Fe. These exhibited certain pronounced and distinct advantages of their own as catalysts. It was found that Pt–Ru/Vulcan carbon powder nanocomposites showed a better DMFC performance than a commercial unsupported $Pt_{50}Ru_{50}$ colloidal catalyst under identical operating conditions [83]. The heterogeneous Pt–Fe/MWNT catalysts prepared by a modified polyol synthesis strategy showed almost twice the catalytic specificity compared with Pt/MWNTs [84]. Moreover, because Pt is very expensive, there is an urge to explore nonplatinic catalysts. Serov and Kwak [85] have reviewed several classes of possible Pt substitutes. They described the transition metal carbides, oxides, alloys and new exotic catalysts as nonplatinic catalysts with a focus on synthetic methods, corrosion stability and activity toward the electrocatalytic oxidation of CH_3OH. Low prices and strong resistance toward poisonous substances are the two major reasons behind the synthesis of such nonplatinic catalysts.

The catalytic activity of catalyst particulates toward CH_3OH oxidation is influenced by several factors, including method of preparation, particle size, carbon functionality, ad-atoms effect and morphology of carbon supports. Liu *et al.* [86] provided an extensive review on three important methods for preparing carbon-supported Pt–Ru catalysts: (i) the impregnation method; (ii) the colloidal method; and (iii) the micro-emulsion method. It was realized that employing simple methods, such as glycol colloidal method and spray pyrolysis method, has resulted in the synthesis of state-of-the-art Pt–Ru/C catalysts. The review [86] also focused on the exploration of new catalyst systems, consisting of low noble metal content and non-noble metal elements, through fast activity down-selection methods, such as the combinatorial method. This method exhibited a strong potential for fast catalyst down-selection and provided a promising catalytic activity compared with the currently best available Pt/Ru catalysts.

On the other hand, CH_3OH-tolerant catalysts, such as metal phthalocyanines, porphyrins, metal oxides, metal carbides and Ru-based chalcogenides were found to have competitive ORR activity; however, their lifetimes need to be improved [87–91]. Various C-supported binary and ternary alloys of Pt, such as Pt–Co/C, Pt–Cr/C, Pt–Ni/C, Pt–Fe/C and Pt–Cr–Co/C showed better performance compared with Pt/C as cathode catalysts in DMFCs [53,88–95]. Lee and Popov [96] provided a short review on the catalytic properties of the selected Ru compounds, including crystalline Chevrel-phase chalcogenides, nanostructured Ru and Ru–Se clusters and Ru–N chelate compounds. Such Ru-based compounds showed high catalytic activity and selectivity owing to the fact that a high number of *d*-states are concentrated in a narrow energy region. The newly developed Se-free Ru/Nx catalysts supported on a high-surface-area carbon provided

cell performance comparable with that of Pt/C catalysts. Li *et al*. [97] prepared a series of nanostructured Pt–Fe/C with varying Pt : Fe ratios by a modified ethylene glycol method and subsequent heat treatment at 900 °C under H/Ar (10 vol.%) atmosphere. DMFC tests showed that the Pt–Fe/C with a Pt : Fe ratio of 1.2:1 exhibited the highest fuel cell performance among all Pt/C and other Pt–Fe/C catalysts under a testing condition of 90 °C cell temperature and 0.2 MPa O_2 back pressure. Under this operating condition, the power density of DMFC obtained with the Pt–Fe/C cathode catalyst reached 120 mW cm^{-2}, while that obtained with the Pt/C cathode catalyst is only 92 mW cm^{-2}. Wang *et al*. [98] developed an MEA with a double-layered catalyst cathode prepared by Pt/Ru-black as the inner catalyst layer and Pt-black as the outer catalyst layer. This new MEA presented a better cell performance than the traditional one. The electrochemical oxidation current due to CH_3OH permeation decreased from 83.5 to 52.7 mA cm^{-2}, while the open-circuit voltage (OCV) increased from 0.594 to 0.641 V.

To increase the DMFC performance, Suo *et al*. [99] prepared a double-catalytic layered MEA consisting of a hydrophilic thin-film layer of inner catalyst and a traditional electrode with an outer catalyst. Pt/Ru-black and Pt-black were used as inner catalysts on the anode and cathode, respectively. The outer catalyst layers were prepared from C-supported Pt/Ru and Pt on the anode and the cathode, respectively. Both catalyst-coated membrane and gas diffusion electrode methods were employed for fabricating a new MEA. The peak density reached a value of 19 mW cm^{-2} at a 2 M CH_3OH concentration under 2 atm O_2 pressure at room temperature. This value was much higher compared with that obtained with traditional MEA. Existence of three gradients in the new MEA, namely catalyst concentration, porosity and hydrophilicity gradients, is responsible for this enhancement.

Although C-supported catalyst systems proved to be superior to pristine catalyst systems in most aspects, they suffer from certain drawbacks and are not 'up to the mark' especially in terms of efficiency. Therefore, in the last couple of years, researchers have focused on graphene as an alternative base material in place of traditionally used carbon, primarily because of its unique and outstanding physicochemical properties, such as an extremely high specific surface area of 2600 m^2 g^{-1}, high electronic conductivity, large surface-to-volume ratio, high stability and low CO poisoning [61,100–106]. Huajie *et al*. [106] developed a new method, called soft chemical method, for loading Pt nanoparticles on graphene nanoplates without damaging the structure of graphene. This composite catalyst exhibited superior electrochemical activity, producing a peak current density value of 57.7 mA cm^{-2} at 2 M CH_3OH concentration, as well as high tolerance toward poisoning during CH_3OH oxidation. Sharma *et al*. [107] reviewed the obtained performances and associated issues regarding catalyst-supporting matrices fabricated using a variety of carbon-based materials, such as CNT, carbon nanofibers (CNF), mesoporous carbon and graphene, as well as noncarbonaceous materials, such as titania, indium oxides, alumina, silica and tungsten oxide and carbide, ceria, zirconia nanostructures and conducting polymers. For example, conducting polymers have evolved as a potential catalyst-supporting material for both electrodes, while being used either individually or in conjunction with CNTs, CNFs, mesoporous carbon and graphene [60,108–112]. Trifluoromethanesulfonic acid-doped polyaniline nanofibers, electrochemically incorporated onto carbon paper, led to a significant improvement in the degree of CH_3OH oxidation. It also resulted in improvements in the accessible surface area, the electronic conductivity, the charge transfer at the polymer/electrolyte interface and the mass transfer resistance [113]. The Pt–Ru catalyst on this modified anode produced a maximum power density of 105 mW cm^{-2}, as compared with a value of 75 mW cm^{-2} obtained for the unmodified anode [114]. On the other hand, the cell performance using a Co/polypyrrole (PPy)–C composite cathode was found to be very stable, showing no appreciable drop after over 100 h of operation [115]. PPy deposition on a Vulcan XC-72 matrix was reported to preferentially block a significant amount of micropores and mesopores initially present within the Vulcan support, resulting in enhancements of both the current and power densities, using both pure oxygen and air feed, leading to improved ORR activity [116]. Again, a Pd/PPy–graphene composite electrode produced an enhanced electrocatalytic oxidation of CH_3OH for DMFCs operating under alkaline conditions [60]. Similarly, modified electrodes consisting of Pt/PPy-MWNTs showed higher catalytic stability than Pt/MWNTs electrode, owing to the synergistic interaction between Pt and the carrier [117].

3.2. Methanol crossover

CH_3OH permeation through the PEM, such as Nafion, is one of the most critical factors affecting the performance of a DMFC. The deleterious phenomenon of CH_3OH crossover significantly reduces the OCV, current density and fuel utilization, resulting in an overall decrease in cell performance. In addition, the crossover creates a mixed potential at the cathode, which leads to cathode depolarization [118–120]. This phenomenon is caused by diffusion and electro-osmotic drag across the membrane. On reaching the cathode, CH_3OH gets oxidized by O_2. With time, the cathode catalyst gets poisoned by the reaction intermediates, such as CO, adsorbed on the catalyst surface, eventually resulting in a decrease in overall cell performance [121,122].

Because the adduct Pt–CO is thermolabile, the catalytic activity toward the electro-oxidation of CH_3OH can be improved by increasing the DMFC operating temperature, which will drastically reduce or eliminate the catalyst poisoning [123,124]. In addition, an increase in the operating temperature improves the ORR at the cathode and proton conductivity through the PEM and hence decreases the polarization effects [125–129]. However, the unwanted

CH_3OH crossover also increases with a rise in temperature. Valdez and Narayanan studied the effect of cell temperature on CH_3OH crossover and found that the crossover phenomenon increased with increasing temperature. Heinzel and Barragán [128] have reviewed the CH_3OH crossover in DMFCs, where they discussed the various parameters influencing CH_3OH crossover, such as CH_3OH concentration, pressure, temperature, membrane thickness and catalyst morphology. It was realized that high temperature and high cathode pressure can improve the cell performance. Therefore, in effect, the CH_3OH crossover gets negatively influenced by the operating temperature; however, an increase in temperature is responsible for realizing a faster reaction rate (i.e., better reaction kinetics) at both electrodes, which in turn increases the cell performance. Again, an increase in CH_3OH crossover, resulting from an increase in the cell operating temperature, leads to lowering of the reaction rate at the cathode. This interdepending and contradictory nature of the situation present in the operation of a DMFC calls for proper optimization of the conditions to be reached, depending upon the requirements of the intended application. The effect of various parameters on CH_3OH crossover and cell performance has been summarized in Table V [128].

Ren *et al*. [130] used lower CH_3OH concentrations and optimized cell design to decrease CH_3OH crossover in their fuel cell systems. Kordesch *et al*. [131] suggested that circulating electrolyte may reduce the CH_3OH crossover. Gurau and Smotkin [132] extensively characterized CH_3OH crossover by gas chromatography at the cathode exhaust and showed that the crossover effect depends on operating parameters including the MEA temperature, CH_3OH solution concentration and flow rate. Zhang and Wang [133] utilized a mathematical model to simulate the effects of various parameters on CH_3OH crossover. Their simulation results showed that CH_3OH crossover increased significantly at low current densities. Eccarius *et al*. [134] also investigated the influence of significant factors such as temperature, anode catalyst layer thickness and CH_3OH concentration on CH_3OH crossover, as well as on overall DMFC performance. Casalegno *et al*. [135] attempted to make an analysis of CH_3OH crossover by measuring cathode CO_2. Their analysis confirmed that CH_3OH crossover influences fuel utilization and fuel cell efficiency. Wang and Wang [136] developed a comprehensive mathematical model for DMFC, in which they included the phenomenon of CH_3OH crossover arising because of diffusion, electro-osmotic drag and pressure gradient mechanisms. They showed that at high current densities, both diffusion and electro-osmotic drag are responsible for CH_3OH crossover, while only diffusion is dominant at low current densities. Garcia *et al*. [137] proposed a one-dimensional, isothermal and single-phase (liquid) model to predict the CH_3OH concentration profiles at the anode backing layer, catalyst layer and PEM. The model accounted for CH_3OH crossover through the cell, as well as the resulting mixed potential developed at the cathode owing to CH_3OH crossover. In order to investigate the two-phase transport behavior through the catalyst layer and to elucidate the mechanism of cathode mixed potential due to oxidation of crossed over CH_3OH, Liu and Wang [138,139] proposed a mathematical model for the DMFC cathode. The model incorporates a two-phase species transport and multistep electrochemical kinetics, including simultaneous O_2 reduction, CH_3OH oxidation and gas-phase chemical reaction. Their predictions on cathode mixed potential showed good agreement with experimental data. Their results indicate that reduction of the cathode layer thickness favors both liquid H_2O removal and O_2 transport through the layer and, hence, results in improved cathode performance. Baxter *et al*. [119] developed a one-dimensional, single-phase, isothermal mathematical model for a liquid-feed DMFC anode in order to predict the amount of CH_3OH crossover through the membrane at different current densities. Apart from the investigation of the effect of operational parameters on CH_3OH crossover and numerical simulations, many research works have been conducted with the purpose of developing new kinds of proton exchange membranes that can potentially mitigate CH_3OH crossover [140–144] and, therefore, increase the cell performance and fuel efficiency.

Recently, Kang *et al*. [145] developed an advanced MEA with anode MPL and cathode air humidification in order to use a high-concentration CH_3OH fuel in a DMFC system. They obtained a maximum power density of $78\,mW\,cm^{-2}$ at a CH_3OH-feed concentration of 8 M and

Table V. Influence of increasing different operating parameters in the CH_3OH crossover and in the fuel cell performance [128]. Copyright © 2009, Elsevier Ltd.

	Nafion® membrane		
	Cell performance		
Parameters	CH_3OH crossover	Low current density	High current density
Cell temperature	Favorable	Favorable	Favorable
Cathode pressure	Unfavorable	Favorable	Favorable
Feed concentration	Favorable	Unfavorable	Favorable
Current density	Unfavorable	Unfavorable	Unfavorable
Membrane thickness	Unfavorable	Favorable	Unfavorable
Membrane equivalent weight	Unfavorable	Favorable	Unfavorable

cell operating temperature of 60 °C. Park *et al*. [146] designed an MEA with multilayer electrodes for a high-concentration CH_3OH operation. This novel MEA was able to produce a maximum power density of 35.1 mW cm^{-2} and could maintain a high power density of 30 mW cm^{-2} at a 0.405 V applied potential under constant current operation. Lufrano *et al*. [147] designed an efficient composite membrane based on sulfonated polysulfone (SPSf) and acidic silica in order to reduce the CH_3OH crossover. This composite membrane showed the lowest crossover current of only 8 mA cm^{-2}, which was 43% lower than that obtained by using a pure SPSf membrane and 33% lower compared with a composite membrane based on bare silica (SPSf–SiO_2).

3.3. Gas and water management

Gas management is an important issue in DMFC design as it greatly influences the performance of fuel cells. CO_2 is produced as a result of CH_3OH electrochemical oxidation at the anode (Reaction 1), and therefore, CO_2 gas bubbles should be removed efficiently in order to prevent blocking of the anode channels. Otherwise, this will lead to limited mass transport and poor distribution of reactants and consequently will decrease the efficiency of the fuel cells. In addition, efficient management of H_2O is also necessary in order to avoid cathode flooding and effectively resolves the issues regarding CH_3OH concentration, power density and the fuel efficiency in a DMFC systems [148–151]. H_2O gets produced at the cathode by the ORR (Reaction 2). Moreover, H_2O gets transported from the aqueous anode to the cathode due to diffusion and electro-osmotic drag. As a consequence, a large amount of H_2O accumulates and causes cathode flooding, thereby reducing the performance of the cell significantly by decreasing the power and stability of a DMFC system. As a remedial measure, the nature of the diffusion layers (also called microporous layers) needs to be improved by controlling the hydrophilicity of the substrate and other associated components that can in turn avoid the flooding and increase the cell performance. Traditionally, a high cathode gas flow rate (high stoichiometry) is applied to prevent H_2O flooding. The parameters that exert control over the H_2O management in a DMFC are temperature, humidity of the inlet air, amount and concentration of fuels, stoichiometry, current density and membrane's H_2O transport properties, such as the coefficients of diffusion and electro-osmotic drag. However, because of the difficulties associated with a detailed experimental investigation of DMFC cells, a number of mathematical models have been proposed that can accurately predict the critical operation conditions required to minimize the problem of H_2O flooding and lend an understanding of the gas–liquid flow behavior, CO_2 evolution and gas dynamics [125,152–156].

Lu and Wang [125] developed a transparent DMFC that has enabled them to visualize two-phase phenomena occurring *in situ*, namely bubble flow at the anode and H_2O flooding at the cathode. To characterize the polarization behavior and to investigate the influence of backing pore structure, two types of MEAs employing Nafion112 as the PEM were used. In one MEA, a Toray carbon paper backing material was used, while a commercially available carbon cloth was used in the other MEA. This investigation revealed that the anode backing layer with uniform pore size and possessing more hydrophilic character is favorably suited for gas management at the anode, while flow visualization analysis indicated that materials having more hydrophobic nature are suitable for H_2O management at the cathode. For a liquid-feed DMFC, Yang and Liang [152] proposed a mathematical model with reduced complexity, involving two significant mass transport phenomena: (i) the two-phase transport effect due to CO_2 generation at the anode; and (ii) the under-rib mass convection effect in the presence of a pressure drop along a single serpentine fuel flow channel. The simulation was focused on the optimization of the flow-field structure and the fuel cell operating parameters including flow rate, CH_3OH concentration and temperature. The results showed that the limiting current density increases with increasing CH_3OH concentration and CH_3OH flow rate at the anode. However, at flow rates above 5 mL min^{-1}, no further improvement was observed. A similar trend can also be expected for power density. It was found that the maximum power density became less remarkable when the CH_3OH concentration was increased beyond 2 M and showed a drop at 6 M concentration. This was explained to occur due to the enhancement in CH_3OH crossover at higher CH_3OH concentration. The results also showed that an increase in temperature results in improved limiting current density and power density values. Celik and Mat [127] analyzed the distribution of CH_3OH and H_2O in a DMFC with the help of an experimental and numerical study. Their mathematical model accounted for fluid flow, species balance, charge transfer and electrochemical reactions. Their results showed that operating temperature is the main parameter affecting the performance of a DMFC, which exhibited a threefold increase upon increase in temperature from 25 to 75 °C. The numerical results further indicated that the CH_3OH concentration decreases along the channel and current density increases close to the channel walls. Rice and Faghri [153] applied a multiphase, multicomponent, thermal and transient model to optimize the H_2O and air management systems for a passive DMFC. They investigated several parameters, such as power density, fuel utilization, energy efficiencies and H_2O balance coefficients. They performed the optimizations of membrane thickness and CH_3OH concentration using both polarization curves and transient simulations. These optimum values were used for the purpose of optimizing the H_2O–air management systems. Their investigations showed that a system that uses two additional cathode GDLs exhibited improved H_2O management, while improvement in gas management occurs for a system that uses an oil-sorbent air filter. These observations were accompanied by increased power density and H_2O balance coefficient. Yang and Zhao [154] studied the influence of flow-field designs on the performance of a DMFC. For this

purpose, they compared the performance of a serpentine flow field with that of a parallel flow field, using a video microscope. They analyzed the effect of flow channel length on cell performance and pressure drop. They reported that for both designs, larger channels yielded a better performance. Yang *et al.* [129] measured a two-phase flow pressure drop in the anode flow field and showed that the pressure drop becomes independent of current density at a high CH_3OH solution flow rate. Argyropoulos *et al.* [151,155] used a transparent DMFC to visualize gas evolution and was perhaps among the first to observe the two-phase flow pattern in the anode channel under various operating conditions. This flow visualization showed that the increase in the liquid phase inlet flow rate facilitates the gas removal from the anode flow channel.

Recently, Yuan *et al.* [157] investigated both numerically and experimentally the effect of anode flow-field designs on the performance of a DMFC by introducing a number of different serpentine channel designs. Their experimental results revealed that the performance of the cell equipped with a double serpentine flow field (19.96 mW cm^{-2}) was better than that having a single (18.11 mW cm^{-2}) or triple flow field (16.20 mW cm^{-2}). Kumar *et al.* [8] established a better coordination between different operating parameters and flow channel designs. It was found that an addition of a small amount (2 M) of phosphoric (36 mW cm^{-2}) and sulfuric acids (42 mW cm^{-2}) in 2 M CH_3OH fuel enhances the performance of a DMFC rapidly while using a double serpentine flow channel and operating up to a temperature of 70 °C. Hsieh *et al.* [158] proposed a new flow-field design, which consisted of one inlet and four outlet systems at both ends of the electrodes (both anode and cathode). They reported a significant reduction in the production of CO_2 gas in the anode flow channels and water in the cathode flow channels (Figure 9).

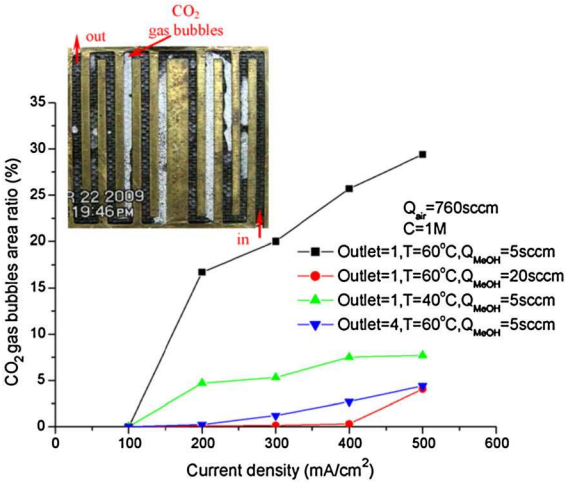

Figure 9. Plots representing the ratio of the area of CO_2 gas bubbles as a function of current density at different temperatures and for different numbers of outlet at different anode flow rates with 1 M methanol concentration. Reprinted from [158], Copyright © 2010, Elsevier.

4. EFFECT OF OPERATING PARAMETERS ON DMFC PERFORMANCE

The performance of a DMFC gets further limited by operational parameters, such as cell temperature, CH_3OH concentration, anode and cathode flow rate, cathode backpressure, cathode humidification temperature and membrane thickness. In order to reduce CH_3OH crossover, improve electrode kinetics and retard cathode flooding, the choice of optimal cell operating parameters plays an important role. Seo and Lee investigated the influence of operating temperature, CH_3OH concentration, CH_3OH flow rate, cathode flow rate and cathode backpressure on CH_3OH crossover and efficiency of a DMFC [156]. For this purpose, they used an MEA having a 5 cm^2 active area and comprising of a Nafion117 membrane, Pt/Ru anode catalyst and Pt cathode catalyst with loadings of 4 mg cm^{-2} in both cases. They subsequently measured the crossover current density under an open-circuit condition, using humidified nitrogen at the cathode. Their measurements showed that the efficiency of a DMFC increases upon increasing the cell temperature and cathode backpressure. It was found that as the CH_3OH concentration increased from 1 to 4 M, the CH_3OH crossover current density increased significantly, resulting in a decrease in OCV and limiting current density. They concluded that 1 M is the optimum CH_3OH concentration required to obtain maximum efficiency. They further observed that the performance and efficiency of a DMFC decrease with the increase of anode flow rate of CH_3OH. However, above a flow rate of 5 mL min^{-1}, no significant changes of these properties were observed. This led them to conclude that at an anode flow rate of 5 mL min^{-1}, maximum crossover takes place. Seo *et al.* [159] further studied the performance characteristics of a DMFC at various operating conditions including cell temperature, CH_3OH concentration, flow rate, cathode humidification temperature and cathode backpressure, using air or O_2 as the oxidant gas. Their results showed that the performance of a DMFC increases with an increase in cell temperature, cathode flow rate and cathode backpressure. They made a comparison of the performance between air and O_2 as the oxidant gas with the help of the polarization curves and showed that the cell using O_2 exhibited superior performance than the one using air. They also presented a discussion on CH_3OH diffusion and transfer conversion rate using the effective mass transfer coefficient and Damköhler number under various performance parameters. The maximum performance obtained for the MEA mentioned earlier appeared corresponding to a cell temperature of 80 °C, anode flow rate of 3 mL min^{-1}, CH_3OH concentration of 1 M, cathode flow rate of 200 cm^3 min^{-1} and a cathode backpressure of 300 kPa. Scott *et al.* [141] developed a mathematical model for DMFC and investigated numerically the

parameters affecting the performance of a single cell. The model incorporated the influence on CH_3OH crossover by a combination of factors, including diffusion, electro-osmotic drag and pressure, variation of reactant concentration and overpotentials in the catalyst layer. The numerical results showed that at high operating temperatures, the values of power density and cell potential measured at fixed current densities increase with a corresponding increase in overall cell performance. The performance also experienced an improvement upon increasing the O_2 pressure at the cathode. To study the influence of the thickness of PEM on the DMFC performance, Silva *et al*. [160] prepared the MEAs by hot pressing the membrane samples between two Etek® ELAT electrodes. Sulfonated poly(ether ether ketone) membranes having a degree of sulfonation of 42% and thicknesses of 25, 40 and 55 μm were tested at several temperatures by evaluating the current–voltage polarization curve, the OCV and the constant voltage current at 35 mV. DMFC test results showed that thinner membranes have lower proton resistance and higher CH_3OH permeation and, therefore, have higher current and power densities due to lower ohmic losses. Meyers and Newman [143,144] proposed a mathematical model to improve the performance of a DMFC. They concluded that for achieving higher fuel efficiency and better cathode performance, CH_3OH concentration should be as low as possible. Furthermore, the membrane thickness should be as thin as can be allowed from mechanical consideration, and the catalyst layer should have a high enough specific surface area in order to obtain maximum performance.

Many research works have been performed to characterize the effect of various operating parameters on the performance of a DMFC [21,141,143,144,156,159–163]. Based on a thorough investigation of available literature, we present a summary of the influence that different operating parameters render on the overall cell performance in the following subsections.

4.1. Cell temperature

A high cell temperature in a DMFC has a negative effect on CH_3OH crossover. As the cell temperature increases, the CH_3OH crossover current density increases. However, the performance of a DMFC increases with an increase in cell temperature owing to higher reaction rates at both electrodes, lower cell resistance and enhanced mass transfer. Accordingly, with an increase in cell temperature, ohmic and activation losses of the fuel cell decrease, owing to the activation of catalytic and electrochemical reactions at the electrodes. Thus, a high operating temperature is valuable for DMFC performance in terms of improvements in active electrochemical reaction at both electrodes. On the other hand, it has an adverse effect on performance owing to high concentration loss caused by increasing CH_3OH crossover by electro-osmotic drag.

4.2. Methanol concentration

With an increase in CH_3OH concentration, the performance of a DMFC decreases because of a corresponding increase in CH_3OH crossover caused by an inactive CH_3OH reaction rate. The CH_3OH crossover gives rise to a mixed potential at the cathode and therefore degrades the performance of a DMFC by lowering the OCV, current density and fuel utilization. However, at high current densities, a lower performance of the cell at a lower concentration of CH_3OH is observed. This occurs probably because of the concentration polarization effects. Hence, it is essential to find an optimal concentration under the operating conditions of a fuel cell.

4.3. Anode flow rate

An increase in anode flow rate leads to a corresponding decrease in the OCV due to an enhancement in CH_3OH permeation through the polymeric membrane. A slow CH_3OH reaction rate against an increasing CH_3OH flow rate results in an incomplete reaction of CH_3OH, and therefore, the amount of CH_3OH increases severely. Thus, both the performance and efficiency of a DMFC decrease because of the concentration loss caused by the CH_3OH crossover along with an increase in CH_3OH flow rate.

4.4. Cathode flow rate

The performance of a DMFC shows an improvement with an increase in the cathode flow rate due to a decrease in concentration loss caused by an active reduction reaction, a high O_2 concentration and protons permeated at the cathode. Moreover, a high cathode flow rate results in oxidation of permeated CH_3OH by enough O_2 present at the cathode and removes the H_2O permeated through the membrane by electro-osmotic drag.

4.5. Cathode backpressure

Cathode backpressure plays an important role in the improvement of the performance of a DMFC. As the cathode backpressure increases, the CH_3OH crossover and electro-osmotic drag decrease owing to increasing O_2 partial pressure at the cathode. Under this condition, the OCV and the limiting current density increase, and consequently, both the performance and efficiency of a DMFC get increased by active reduction reaction caused by increasing O_2 residence time corresponding to the high cathode backpressure.

4.6. Cathode humidification temperature

An increase of humidification temperature may induce a high relative humidity of the reactant gas. So, the O_2 partial pressure reduces, and the excessive H_2O retards the mass transfer on the electrode at the region of high current density, and hence, the overall cell performance experiences a decrease. On the contrary, a low humidification

temperature of the reactant gas fails to hydrate the membrane sufficiently, and consequently, the cell performance decreases because of the low ionic conductivity. Therefore, it is important to determine the optimum cathode humidification temperature in order to realize the maximum cell performance.

4.7. Membrane thickness

As the membrane thickness increases, the CH_3OH crossover decreases, and hence, an increase in OCV is expected. However, at high current densities, this trend gets altered because under such conditions, membrane resistance to transport phenomena becomes dominant. Therefore, thicker membranes exhibit some enhancement of the cell voltage owing to reduced crossover but tend to have higher resistances, leading to degradation of the cell performance. With a decrease in membrane thickness, the resistance toward charge transfer from the anode to the cathode reduces, and the reduction of concentration polarization in the polymer is observed. Thus, the performance of a DMFC is probably determined by the combined effects of ionic conductivity and fuel crossover.

5. DMFC POLARIZATION BEHAVIORS AND EFFICIENCY

The performance of a DMFC is usually determined by measuring the polarization curve, where cell voltage is plotted as a function of current density. From Figure 10, by representing a typical polarization curve, it can be seen that the curve is typically S shaped and reflects the different limiting factors that occur during the operation of a fuel cell. From the figure, it is clear that the cell exhibits the maximum experimental voltage or OCV value at zero current density. However, the experimental OCV differs from the reversible DMFC voltage because of overpotentials, arising mainly because of fuel losses. Performance losses caused by sluggish kinetics, ohmic resistances and mass transport can all be predicted from such a polarization curve [164]. At low current densities,

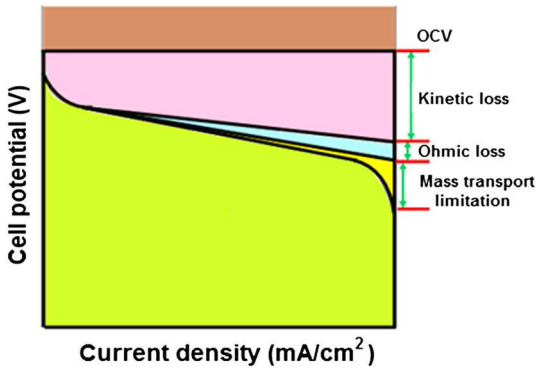

Figure 10. A typical polarization curve used to determine the performance of a direct methanol fuel cell.

the performance of a DMFC is mostly limited by the slow kinetics of the electrochemical reactions occurring at the electrodes. Such a type of voltage losses caused by reduced kinetics is called the activation overpotential (η_{act}), and this is represented by a sharp drop in potential at low current densities. These limitations can generally be overcome by employing an 'activation catalyst' and by increasing the temperature. The ohmic overpotential (η_{Ohm}) caused by the resistive losses within a DMFC system (from the membrane/electrode resistances) becomes significant at intermediate current densities. The ohmic losses are usually indicated by the linear region obtained at medium current densities in a polarization curve. Generally, it is considered that a reduction in the thickness of the electrolyte layer between anode and cathode would eliminate ohmic overpotential.

Mass transport losses are observed at high current densities because of the slow mass transport of the reactants at the electrode/electrolyte interface. This type of voltage loss is termed as concentration overpotential (η_{conc}) and represented by a sudden drop in potential at high current densities in the polarization curve. The concentration overpotential depends upon several factors, such as the porosity of the materials that influence the gas or liquid flow or the permeability of the membrane involved in the ionic flow. The actual cell voltage (V_{cell}) can be obtained from the following equation:

$$V_{cell} = E - \eta_{act} - \eta_{conc} - IR \tag{9}$$

where E is the potential difference between the two electrodes and IR represents ohmic losses.

In order to combine the effects of fuel cell polarization and CH_3OH crossover, the measurement of the efficiency of DMFC becomes a critical factor. The potential efficiency (η_E), which is also called the voltage efficiency, is used to study the fuel cell polarization loss behavior and determined as a function of cell current density from polarization curves according to the following equation:

$$\eta_E = V_{cell}/V_{Th} \tag{10}$$

where V_{cell} is the cell voltage at a specific current density and V_{Th} is the reversible cell voltage, that is, the theoretical maximum cell voltage (1.21 V at 25 °C) based on free-energy change of the overall reaction. The maximum cell voltage, V_{Th}, is obtained as

$$V_{Th} = -nG_R/zF = -(nH_R - TnS_R)/zF \tag{11}$$

where ΔG_R represents the change in Gibb's free energy, ΔH_R represents the overall reaction enthalpy at standard conditions, ΔS_R corresponds to the variation of the system's entropy under standard states, T is the system's absolute temperature, z represents the number of electrons involved in the electrochemical reaction ($z = 6$ for DMFC) and F is the Faraday constant (96,484.6 C mol^{-1}).

Table VI. Remedy and possible future directions that can lead to overcoming of the critical drawbacks associated with direct methanol fuel cell and can increase its commercialization prospects.

Limitation	Remedy	Future directions
Low power density	To enhance the oxidation kinetics	Multifunctional catalysts (Pt-based alloy)
		Increase the operating temperature and pH
	To improve the electrode performance	Highly dispersed catalysts (nanoparticle)
		Thin-film electrodes
		Optimization of the MEA
		Nanocomposite bipolar plate
Methanol crossover	To fabricate membranes impermeable to methanol	Anion exchange membranes
		Composite membranes
		Polyarylsulfonic membranes
		PVdF/PVdF-HFP-based membranes
	To utilize methanol-tolerant oxygen reduction catalysts	Chevrel-phase type ($Mo_4Ru_2Se_8$), transition metal sulfides ($Mo_xRu_yS_z$, $Mo_xRh_yS_z$) or other transition metal chalcogenides
		Pt-based alloys
High cost	To reduce noble metal loading	Non-noble metal catalysts (without Pt)
		Oxide catalysts
		Cathode catalysts based on iron or cobalt organic macrocycles (phenylporphyrins or phthalocyanines)
		Co/PPy–C
		Decoration (anode catalyst)
	To develop PEM materials as total/partial replacements of Nafion	Anion exchange membranes
		Grafted membranes
		Membranes based on PEEK, SPSf, PVdF-HFP, PBI and so on

MEA, membrane electrode assembly; PEM, polymer electrolyte membrane; PPy, polypyrrole; SPSf, sulfonated polysulfone; PVdF, Polyvinylidene fluoride; PVdF-HFP, Poly (vinylidenefluoride-co-hexafluoro propylene); PEEK, Polyetheretherketone; PBI, Polybenzimidazole.

On the other hand, in order to study the effect of CH_3OH crossover, researchers usually measure the DMFC's Faraday efficiency (η_F), which is also called the fuel efficiency. The Faraday efficiency is defined as the ratio of the converted fuel required to generate electric power (anode) to the total amount of CH_3OH consumed by the system owing to reactions at the anode and CH_3OH crossover. This, however, ignores the possible fuel lost because of CO_2 exhaustion from the anode and unreacted CH_3OH at the cathode. Nevertheless, the effect of these loss mechanisms is small compared with the effect rendered by CH_3OH reacting at the electrodes. The Faraday efficiency (η_F) can be expressed as

$$\eta_F = i_{cell}/(i_{cell} + i_{xover}) \tag{12}$$

where i_{cell} is the DMFC's measured current density and i_{xover} is the current density loss due to CH_3OH crossover. The i_{xover} can be evaluated from the following equation:

$$i_{xover} = \left[N_{CO_2}^{MeOH} \times 6 \times F\right] \Big/ A_{cell} \tag{13}$$

where $N_{CO_2}^{MeOH}$ represents the molar flow rate of CO_2 arising because of parasitic CH_3OH oxidation at the cathode and A_{cell} is the effective area of the DMFC.

The overall efficiency of a cell can be obtained from the product of the potential efficiency (η_E), the Faraday efficiency (η_F) and the thermodynamic efficiency (η_{th}). The thermodynamic efficiency, which is defined as $\Delta G_R/\Delta H_R$, is a constant and independent of the material. Therefore, by neglecting this term, the overall efficiency can be expressed as

$$\eta_{overall} = \eta_E \times \eta_F \tag{14}$$

This equation accounts for both cell polarization and CH_3OH crossover.

6. FUTURE PERSPECTIVES

Despite several years of active research focused on overcoming the sluggishness of the electrode reactions, it still remains as a major challenge. However, use of alternative catalyst systems discussed in this review, along with a proper selection of the supporting-matrix materials, has shown promising results. In our view, use of dispersed micrometal/nanometal particles supported on high-surface-area materials, such as conducting polymers, CNTs, CNFs, graphene and so on, holds the key for realizing practically viable electrode kinetics.

Because CH_3OH crossover poses a major limitation toward the commercialization aspects of DMFCs, researchers have tried to develop an alternative membrane technology and stack/cell design in order to minimize this effect. Blends and composites of both fluorinated and nonfluorinated polymers, especially those based on poly (vinylidene fluoride-co-hexafluoro propylene) (PVdF-*co*-HFP), polyetheretherketone (PEEK), polysulfone and polybenzimidazole (PBI), appear to be prospective DMFC membranes by virtue of possessing lower CH_3OH permeability than Nafion, along with a high enough proton conductivity. In addition, studies on the influence of different operating parameters on CH_3OH crossover reveal that employment of high temperatures and high cathode pressures leads to a reduction in crossover while improving the cell performance.

Finally, the expensive nature of a DMFC operation, primarily because of the high cost of constituting materials, such as Pt and Nafion, is another critical parameter preventing this device from getting successfully commercialized. One possible way of overcoming this particular problem is by the partial or total replacement of these costly materials by other prospective candidates. However, it should be remembered that commercialization also demands a practical performance level to be maintained. Therefore, judicious and optimized use of the different available materials is important. At present, although partial replacement strategies of the costly materials seem to be the most viable option; however, total replacements are increasingly being reported. Nevertheless, in our view, use of nanodimensional Pt-based alloys, use of high-surface-area catalyst supports for better anchoring, dispersion and utilization of the costly Pt and use of cheap and effective PEM materials (mentioned earlier) should lead to better and cheap DMFC operation. A summary of remedies and possible future directions that can lead to overcoming of the critical drawbacks associated with direct methanol fuel cell is presented in Table VI.

7. CONCLUSION

Direct methanol fuel cell technology has been deemed as the next big thing in the field of alternative power sources and has shown signs of potentialities to replace conventional batteries in application in portable electronic devices. However, despite several years of active research, there still exist several drawbacks associated with its basic operation, which are preventing the widespread use of this potentially promising technology. In this review, we focused on these drawbacks and tried to identify and critically scrutinize the various factors and parameters associated with these drawbacks. We discussed the effects rendered by various operating parameters, namely cell temperature, membrane thickness, cathode backpressure, electrode flow rate, CH_3OH concentration and cathode humidification temperature, on the performance of a DMFC. We also focused on various approaches made to overcome these drawbacks. Few examples are as follows: (i) development of dispersed micrometal/nanometal particles supported on high-surface-area materials as catalysts led to enhanced efficiency of the catalysts; (ii) use of nonplatinic catalysts led to low prices and strong resistance toward poisonous substances such as CO; (iii) CH_3OH-tolerant catalysts were found to have competitive ORR activity with that of conventional Pt; (iv) voltage losses occurring owing to activation overpotential can be countered by employing an 'activation catalyst' and by increasing the temperature; (v) ohmic overpotential losses can be eliminated by reducing the thickness of the electrolyte layer between anode and cathode; and (vi) concentration overpotential losses can be optimized by adjusting the permeability and porosity of the membrane. Different limitations of DMFCs, their causes and the approaches adopted for solving these problems have been presented in Table IV. We, in our laboratory, are also involved in the research and developmental aspects of DMFC and are working toward the objective of making this technology practically and commercially realizable [6,8,28,165,166].

ACKNOWLEDGEMENTS

P. P. K. would like to thank the Ministry of New and Renewable Energy for a grant-in-aid. P. K. thanks the Department of Science and Technology, Government of India, for an INSPIRE Fellowship. K. D. is thankful to the Council of Scientific and Industrial Research, India, for a Senior Research Fellowship.

REFERENCES

1. Grove WR. On voltaic series and the combination of gases by platinum. *Philosophical Magazine Series 3* 1839; **14**:127–130.
2. Aricò AS, Srinivasan S, Antonucci V. DMFCs: from fundamental aspects to technology development. *Fuel Cells* 2001; **1**:133–161.
3. Rice C, Ha S, Masel RI, Waszczuk P, Wieckowski A, Barnard T. Direct formic acid fuel cells. *Journal of Power Sources* 2002; **111**:83–89.
4. Morse JD. Micro-fuel cell power sources. *International Journal of Energy Research* 2007; **31**:576–602.
5. Ahmed M, Dincer I. A review on methanol crossover in direct methanol fuel cells: challenges and achievements. *International Journal of Energy Research* 2011; **35**:1213–1228.
6. Das S, Kumar P, Dutta K, Kundu PP. Partial sulfonation of PVdF-*co*-HFP: a preliminary study and characterization for application in direct methanol fuel cell. *Applied Energy* 2014; **113**:169–177.
7. Bullen RA, Arnot TC, Lakeman JB, Walsh FC. Biofuel cells and their development. *Biosensors and Bioelectronics* 2006; **21**:2015–2045.

8. Kumar P, Dutta K, Kundu PP. Enhanced performance of direct methanol fuel cells: a study on the combined effect of various supporting electrolytes, flow channel designs and operating temperatures. *International Journal of Energy Research* 2013. doi:10.1002/er.3034.
9. Cho YK, Donohue TJ, Tejedor I, Anderson MA, McMohan KD, Noguera DR. Development of a solar-powered microbial fuel cell. *Journal of Applied Microbiology* 2008; **104**:640–650.
10. Liu BH, Li ZP. Current status and progress of direct borohydride fuel cell technology development. *Journal of Power Sources* 2009; **187**:291–297.
11. Shukla AK, Raman RK. Methanol-resistant oxygen-reduction catalysts for direct methanol fuel cells. *Annual Review of Materials Research* 2003; **33**:155–168.
12. Joon K. Fuel cells—a 21st century power system. *Journal of Power Sources* 1998; **71**:12–18.
13. Lovley DR. Microbial fuel cells: novel microbial physiologies and engineering approaches. *Current Opinion in Biotechnology* 2006; **17**:327–332.
14. Davis F, Higson SPJ. Biofuel cells—recent advances and applications. *Biosensors and Bioelectronics* 2007; **22**:1224–1235.
15. Rosen MA, Dincer I. On exergy and environmental impact. *International Journal of Energy Research* 1997; **21**:643–654.
16. Mo Z-J, Zhu X-J, Wei L-Y, Cao G-Y. Parameter optimization for a PEMFC model with a hybrid genetic algorithm. *International Journal of Energy Research* 2006; **30**:585–597.
17. Qian W, Wilkinson DP, Shen J, Wang H, Zhang J. Architecture for portable direct liquid fuel cells. *Journal of Power Sources* 2006; **154**:202–213.
18. Höhlein B, von Andrian S, Grube T, Menzer R. Critical assessment of power trains with fuel-cell systems and different fuels. *Journal of Power Sources* 2000; **86**:243–249.
19. Cheng X, Shi Z, Glass N, Zhang L, Zhang J, Song D, Liu Z-S, Wang H, Shen J. A review of PEM hydrogen fuel cell contamination: impacts, mechanisms, and mitigation. *Journal of Power Sources* 2007; **165**:739–756.
20. Mori D, Hirose K. Recent challenges of hydrogen storage technologies for fuel cell vehicles. *International Journal of Hydrogen Energy* 2009; **34**:4569–4574.
21. Liu JG, Zhao TS, Chen R, Wong CW. The effect of methanol concentration on the performance of a passive DMFC. *Electrochemistry Communications* 2005; **7**:288–294.
22. Dillon R, Srinivasan S, Aricò AS, Antonucci V. International activities in DMFC R&D: status of technologies and potential applications. *Journal of Power Sources* 2004; **127**:112–126.
23. Sv A, Meusinger J. Process analysis of a liquid-feed direct methanol fuel cell system. *Journal of Power Sources* 2000; **91**:193–201.
24. Yao KZ, Karan K, McAuley KB, Oosthuizen P, Peppley B, Xie T. A review of mathematical models for hydrogen and direct methanol polymer electrolyte membrane fuel cells. *Fuel Cells* 2004; **4**:3–29.
25. Lindermeir A, Rosenthal G, Kunz U, Hoffmann U. On the question of MEA preparation for DMFCs. *Journal of Power Sources* 2004; **129**:180–187.
26. Firtına I, Guner S, Albostan A. Preparation and characterization of membrane electrode assembly (MEA) for PEMFC. *International Journal of Energy Research* 2011; **35**:146–152.
27. Aricò AS, Creti P, Giordano N, Antonucci V, Antonucci PL, Chuvilin A. Chemical and morphological characterization of a direct methanol fuel cell based on a quaternary Pt–Ru–Sn–W/C anode. *Journal of Applied Electrochemistry* 1996; **26**:959–967.
28. Jung H-Y, Cho K-Y, Lee YM, Park J-K, Choi J-H, Sung Y-E. Influence of annealing of membrane electrode assembly (MEA) on performance of direct methanol fuel cell (DMFC). *Journal of Power Sources* 2007; **163**:952–956.
29. Tang H, Wang S, Pana M, Jiang SP, Ruan Y. Performance of direct methanol fuel cells prepared by hot-pressed MEA and catalyst-coated membrane (CCM). *Electrochimica Acta* 2007; **52**:3714–3718.
30. Krishnan NN, Prabhuram J, Hong YT, Kim H-J, Yoon K, Ha H-Y, Lim T-H, Kim S-K. Fabrication of MEA with hydrocarbon based membranes using low temperature decal method for DMFC. *International Journal of Hydrogen Energy* 2010; **35**:5647–5655.
31. Wan N, Mao Z, Wang C, Wang G. Performance of an integrated composite membrane electrode assembly in DMFC. *Journal of Power Sources* 2007; **163**:725–730.
32. Kundu PP, Kim BT, Ahn JE, Han HS, Shul YG. Formation and evaluation of semi-IPN of Nafion 117 membrane for direct methanol fuel cell 1. Crosslinked sulfonated polystyrene in the pores of nafion 117. *Journal of Power Sources* 2007; **171**:86–91.
33. Boxall DL, Deluga GA, Kenik EA, King WD, Lukehart CM. Rapid synthesis of a Pt_1Ru_1/carbon nanocomposite using microwave irradiation: a DMFC anode catalyst of high relative performance. *Chemistry of Materials* 2001; **13**:891–900.
34. Baschuk JJ, Li X. Carbon monoxide poisoning of proton exchange membrane fuel cells. *International Journal of Energy Research* 2001; **25**:695–713.

35. Oedegaard A, Hebling C, Schmitz A, Møller-Holst S, Tunold R. Influence of diffusion layer properties on low temperature DMFC. *Journal of Power Sources* 2004; **127**:187–196.
36. Krishnamurthy B, Deepalochani S. Effect of PTFE content on the performance of a direct methanol fuel cell. *International Journal of Hydrogen Energy* 2009; **34**:446–452.
37. Zhang J, Yin GP, Lai QZ, Wang ZB, Cai KD, Liu P. The influence of anode gas diffusion layer on the performance of low temperature DMFC. *Journal of Power Sources* 2007; **168**:453–8.
38. Jian-hua T, Zhao-yuan S, Jin-song S, Zhong-qiang S. Preparation of water management layer and effects of its composition on performance of PEMFCs. *Energy Conversion and Management* 2008; **49**:1500–1505.
39. Lin C, Wang T, Ye F, Fang Y, Wang X. Effects of microporous layer preparation on the performance of a direct methanol fuel cell. *Electrochemistry Communications* 2008; **10**:255–258.
40. Park J-Y, Kim H-T, Lee ES, Son I-H, Han S. Effect of the porous carbon layer in the cathode gas diffusion media on direct methanol fuel cell performances. *International Journal of Hydrogen Energy* 2009; **34**:8257–8262.
41. Radhakrishnan V, Haridoss P. Differences in structure and property of carbon paper and carbon cloth diffusion media and their impact on proton exchange membrane fuel cell flow field design. *Materials and Design* 2011; **32**:861–868.
42. Kianimanesh A, Yu B, Yang Q, Freiheit T, Xue D, Park SS. Investigation of bipolar plate geometry on direct methanol fuel cell performance. *International Journal of Hydrogen Energy* 2012; **37**:18403–18411.
43. Chen W, Liu Y, Xin Q. Evaluation of a compression molded composite bipolar plate for direct methanol fuel cell. *International Journal of Hydrogen Energy* 2010; **35**:3783–3788.
44. Kunz HR, Bonville L, Zaffou R, Jiang R, Fenton J. Bipolar plate for fuel cell. US Patent# 8,097,385, 2012.
45. Huang I-B. Evaluation of silver-coated stainless steel bipolar plates for fuel cell applications. *Journal of Power Sources* 2011; **196**:7649–7653.
46. Park T, Chang I, Lee YH, Cha SW. Fabrication of bipolar plates based on graphite sheet via stamping method. *ECS Transactions* 2013; **50**:795–804.
47. Mehta V. Joyce Smith Cooper. Review and analysis of PEM fuel cell design and manufacturing. *Journal of Power Sources* 2003; **114**:32–53.
48. Taherian R, Nasr M. Performance and material selection of nanocomposites bipolar plate in proton exchange membrane fuel cells. *Int. J. Energy Res.* 2013. doi:10.1002/er.3109.
49. Kamarudin SK, Achmad F, Daud WRW. Overview on the application of direct methanol fuel cell (DMFC) for portable electronic devices. *International Journal of Hydrogen Energy* 2009; **34**:6902–6916.
50. Xu C, Zhao TS, Ye Q. Effect of anode backing layer on the cell performance of a direct methanol fuel cell. *Electrochimica Acta* 2006; **51**:5524–5531.
51. Gibbons RM. Silicon rubber gasket and material. US Patent# 4,580,794, 1986.
52. Lai Q-Z, Yin G-P, Wang Z-B. Effect of anode current collector on the performance of passive direct methanol fuel cells. *International Journal of Energy Research* 2009; **33**:719–727.
53. Yousefi S, Ganji DD. Experimental investigation of a passive direct methanol fuel cell with 100 cm^2 active areas. *Electrochimica Acta* 2012; **85**:693–699.
54. Li W, Zhou W, Li H, Zhou Z, Zhou B, Sun G, Xin Q. Nano-structured Pt–Fe/C as cathode catalyst in direct methanol fuel cell. *Electrochimica Acta* 2004; **49**:1045–1055.
55. Mazumder V, Lee Y, Sun S. Recent development of active nanoparticle catalysts for fuel cell reactions. *Advanced Functional Materials* 2010; **20**:1224–1231.
56. Liu F, Wang C-Y. Mixed potential in a direct methanol fuel cell: modeling and experiments. *Journal of the Electrochemical Society* 2007; **154**:B514–B522.
57. Li W, Liang C, Zhou W, Qiu J, Zhou Z, Sun G, Xin Q. Preparation and characterization of multiwalled carbon nanotube-supported platinum for cathode catalysts of direct methanol fuel cells. *The Journal of Physical Chemistry B* 2003; **107**:6292–6299.
58. Yuan W, Scott K, Cheng H. Fabrication and evaluation of Pt–Fe alloys as methanol tolerant cathode materials for direct methanol fuel cells. *Journal of Power Sources* 2006; **163**:323–329.
59. Zainoodin AM, Kamarudin SK, Daud WRW. Electrode in direct methanol fuel cells. *International Journal of Hydrogen Energy* 2010; **35**:4606–4621.
60. Zhao Y, Zhan L, Tian J, Nie S, Ning Z. Enhanced electrocatalytic oxidation of methanol on Pd/polypyrrole–graphene in alkaline medium. *Electrochimica Acta* 2011; **56**:1967–1972.
61. Li Y, Gao W, Ci L, Wang C, Ajayan PM. Catalytic performance of Pt nanoparticles on reduced graphene oxide for methanol electro-oxidation. *Carbon* 2010; **48**:1124–1130.
62. Wu Y-N, Liao S-J, Guo H-F, Hao X-Y. High-performance Pd@PtRu/C catalyst for the anodic oxidation of methanol prepared by decorating Pd/C with a PtRu shell. *Journal of Power Sources* 2013; **224**:66–71.

63. Chakraborty D, Chorkendorff IB, Johannessen T. Metamorphosis of the mixed phase PtRu anode catalyst for direct methanol fuel cells after exposure of methanol: in situ and ex situ characterizations. *Journal of Power Sources* 2007; **173**:110–120.
64. Vidaković T, Christov M, Sundmacher K. Rate expression for electrochemical oxidation of methanol on a direct methanol fuel cell anode. *Journal of Electroanalytical Chemistry* 2005; **580**:105–121.
65. Schultz T, Krewer U, Vidaković T, Pfafferodt M, Christov M, Sundmacher K. Systematic analysis of the direct methanol fuel cell. *Journal of Applied Electrochemistry* 2007; **37**:111–119.
66. Lin Y, Cui X, Ye X. Electrocatalytic reactivity for oxygen reduction of palladium-modified carbon nanotubes synthesized in supercritical fluid. *Electrochemistry Communications* 2005; **7**:267–274.
67. Shukla AK, Raman RK, Scott K. Advances in mixed-reactant fuel cells. *Fuel Cells* 2005; **5**:436–447.
68. Aricò AS, Baglio V, Blasi AD, Modica E, Antonucci PL, Antonucci V. Analysis of the high-temperature methanol oxidation behaviour at carbon-supported Pt–Ru catalysts. *Journal of Electroanalytical Chemistry* 2003; **557**:167–176.
69. Moore JT, Chu D, Jiang R, Deluga GA, Lukehart CM. Synthesis and characterization of Os and Pt–Os/carbon nanocomposites and their relative performance as methanol electrooxidation catalysts. *Chemistry of Materials* 2003; **15**:1119–1124.
70. Colmati F, Antolini E, Gonzalez ER. Pt–Sn/C electrocatalysts for methanol oxidation synthesized by reduction with formic acid. *Electrochimica Acta* 2005; **50**:5496–5503.
71. Kwiatkowski KC, Milne SB, Mukerjee S, Lukehart CM. Synthesis of Pt–Mo/carbon nanocomposites from single-source molecular precursors: a (1:1) PtMo/C PEMFC anode catalyst exhibiting CO tolerance. *Journal of Cluster Science* 2005; **16**:251–272.
72. Kua J, Goddard WA III. Oxidation of methanol on 2nd and 3rd row group VIII transition metals (Pt, Ir, Os, Pd, Rh, and Ru): application to direct methanol fuel cells. *Journal of the American Chemical Society* 1999; **121**:10928–10941.
73. Aricò AS, Poltarzewski Z, Kim H, Morana A, Giordano N, Antonucci V. Investigation of a carbon-supported quaternary Pt–Ru–Sn–W catalyst for direct methanol fuel cells. *Journal of Power Sources* 1995; **55**:159–166.
74. Chu YH, Shul YG. Combinatorial investigation of Pt–Ru–Sn alloys as an anode electrocatalysts for direct alcohol fuel cells. *International Journal of Hydrogen Energy* 2010; **35**:11261–11270.
75. Steigerwalt ES, Deluga GA, Lukehart CM. Pt–Ru/carbon fiber nanocomposites: synthesis, characterization, and performance as anode catalysts of direct methanol fuel cells. A search for exceptional performance. *The Journal of Physical Chemistry B* 2002; **106**:760–766.
76. Dinh HN, Ren X, Garzon FH, Zelenay P, Gottesfeld S. Electrocatalysis in direct methanol fuel cells: in-situ probing of PtRu anode catalyst surfaces. *Journal of Electroanalytical Chemistry* 2000; **491**:222–233.
77. Lizcano-Valbuena WH, Paganin VA, Gonzalez ER. Methanol electro-oxidation on gas diffusion electrodes prepared with Pt-Ru/C catalysts. *Electrochimica Acta* 2002; **47**:3715–3722.
78. Mu Y, Liang H, Hu J, Jiang L, Wan L. Controllable Pt nanoparticle deposition on carbon nanotubes as an anode catalyst for direct methanol fuel cells. *The Journal of Physical Chemistry B* 2005; **109**:22212–22216.
79. Yoo E, Okada T, Kizuka T, Nakamura J. Effect of carbon substrate materials as a Pt–Ru catalyst support on the performance of direct methanol fuel cells. *Journal of Power Sources* 2008; **180**:221–226.
80. Schlange A, dos Santos AR, Hasse B, Etzold BJM, Kunz U, Turek T. Titanium carbide-derived carbon as a novel support for platinum catalysts in direct methanol fuel cell application. *Journal of Power Sources* 2012; **199**:22–28.
81. Zhou C, Wang H, Peng F, Liang J, Yu H, Yang J. MnO_2/CNT supported Pt and PtRu nanocatalysts for direct methanol fuel cells. *Langmuir* 2009; **25**:7711–7717.
82. Xu C, Li Q, Liu Y, Wang J, Geng H. Hierarchical nanoporous PtFe alloy with multimodal size distributions and its catalytic performance toward methanol electrooxidation. *Langmuir* 2012; **28**:1886–1892.
83. Steigerwalt ES, Deluga GA, Cliffel DE, Lukehart CM. A Pt-Ru/graphitic carbon nanofiber nanocomposite exhibiting high relative performance as a direct-methanol fuel cell anode catalyst. *The Journal of Physical Chemistry B* 2001; **105**:8097–8101.
84. Xu K, Pierce DT, Li A, Zhao JX. Nanocatalysts in direct methanol fuel cell applications. *Synthesis and Reactivity in Inorganic, Metal-Organic, and Nano-Metal Chemistry* 2008; **38**:394–399.
85. Serov A, Kwak C. Review of non-platinum anode catalysts for DMFC and PEMFC application. *Applied Catalysis B: Environmental* 2009; **90**:313–320.
86. Liu H, Song C, Zhang L, Zhang J, Wang H, Wilkinson DP. A review of anode catalysis in the direct methanol fuel cell. *Journal of Power Sources* 2006; **155**:95–110.

87. Lu Y, Reddy RG. The electrochemical behavior of cobalt phthalocyanine/platinum as methanol-resistant oxygen-reduction electrocatalysts for DMFC. *Electrochimica Acta* 2007; **52**:2562–2569.
88. Baranton S, Coutanceau C, Roux C, Hahn F, Léger J-M. Oxygen reduction reaction in acid medium at iron phthalocyanine dispersed on high surface area carbon substrate: tolerance to methanol, stability and kinetics. *Journal of Electroanalytical Chemistry* 2005; **577**:223–234.
89. Serov AA, Min M, Chai G, Han S, Seo SJ, Park Y, Kim H, Kwak C. Electroreduction of oxygen over iron macrocyclic catalysts for DMFC applications. *Journal of Applied Electrochemistry* 2009; **39**:1509–1516.
90. Meng H, Shen PK. The beneficial effect of the addition of tungsten carbides to Pt catalysts on the oxygen electroreduction. *Chemical Communications* 2005:4408–4410.
91. Meng H, Shen PK. Tungsten carbide nanocrystal promoted Pt/C electrocatalysts for oxygen reduction. *The Journal of Physical Chemistry B* 2005; **109**:22705–22709.
92. Salgado JRC, Antolini E, Gonzalez ER. Carbon supported Pt–Co alloys as methanol-resistant oxygen-reduction electrocatalysts for direct methanol fuel cells. *Applied Catalysis B: Environmental* 2005; **57**:283–290.
93. Antolini E, Salgado JRC, dos Santos AM, Gonzalez ER. Carbon-supported Pt–Ni alloys prepared by the borohydride method as electrocatalysts for DMFCs. *Electrochemical and Solid-State Letters* 2005; **8**: A226–A230.
94. Antolini E, Salgado JRC, Santos LGRA, Garcia G, Ticianelli EA, Pastor E, Gonzalez ER. Carbon supported Pt–Cr alloys as oxygen-reduction catalysts for direct methanol fuel cells. *Journal of Applied Electrochemistry* 2006; **36**:355–362.
95. Yang H, Alonso-Vante N, Lamy C, Akins DL. High methanol tolerance of carbon-supported Pt–Cr alloy nanoparticle electrocatalysts for oxygen reduction. *Journal of the Electrochemical Society* 2005; **152**: A704–A709.
96. Lee J-W, Popov BN. Ruthenium-based electrocatalysts for oxygen reduction reaction—a review. *Journal of Solid State Electrochemistry* 2007; **11**:1355–1364.
97. Li W, Xin Q, Yan Y. Nanostructured Pt–Fe/C cathode catalysts for direct methanol fuel cell: the effect of catalyst composition. *International Journal of Hydrogen Energy* 2010; **35**:2530–2538.
98. Wang T, Lin C, Ye F, Fang Y, Li J, Wang X. MEA with double-layered catalyst cathode to mitigate methanol crossover in DMFC. *Electrochemistry Communications* 2008; **10**:1261–1263.
99. Suo C, Liu X, Tang XC, Zhang Y, Zhang B, Zhang P. A novel MEA architecture for improving the performance of a DMFC. *Electrochemistry Communications* 2008; **10**:1606–1609.
100. Novoselov KS, Geim AK, Morozov SV, Jiang D, Zhang Y, Dubonos SV, Grigorieva IV, Firsov AA. Electric field effect in atomically thin carbon films. *Science* 2004; **306**:666–669.
101. Geim AK, Novoselov KS. The rise of graphene. *Nature Materials* 2007; **6**:183–191.
102. Li D, Müller MB, Gilje S, Kaner RB, Wallace GG. Processable aqueous dispersions of graphene nanosheets. *Nature Nanotechnology* 2008; **3**:101–105.
103. Stankovich S, Dikin DA, Dommett GHB, Kohlhaas KM, Zimney EJ, Stach EA, Piner RD, Nguyen ST, Ruoff RS. Graphene-based composite materials. *Nature* 2006; **442**:282–286.
104. Xu C, Wang X, Zhu J. Graphene-metal particle nanocomposites. *The Journal of Physical Chemistry C* 2008; **112**:19841–19845.
105. Muszynski R, Seger B, Kamat PV. Decorating graphene sheets with gold nanoparticles. *The Journal of Physical Chemistry C* 2008; **112**:5263–5266.
106. Huang H, Chen H, Sun D, Wang X. Graphene nanoplate–Pt composite as a high performance electrocatalyst for direct methanol fuel cells. *Journal of Power Sources* 2012; **204**:46–52.
107. Sharma S, Pollet BG. Support materials for PEMFC and DMFC electrocatalysts—a review. *Journal of Power Sources* 2012; **208**:96–119.
108. He D, Zeng C, Xu C, Cheng N, Li H, Mu S, Pan M. Polyaniline-functionalized carbon nanotube supported platinum catalysts. *Langmuir* 2011; **27**:5582–5588.
109. Xu YT, Lin SJ, Peng XL, Luo W-A, Gal J-Y, Dai LZ. *In situ* chemical fabrication of polyaniline/multi-walled carbon nanotubes composites as supports of Pt for methanol electrooxidation. *Science China Chemistry* 2010; **53**:2006–2014.
110. Cui Z, Guo CX, Li CM. Self-assembled phosphomolybdic acid-polyaniline-graphene composite-supported efficient catalyst towards methanol oxidation. *Journal of Materials Chemistry A* 2013; **1**:6687–6692.
111. Bai Z, Shi M, Niu L, Li Z, Jiang L, Yang L. A facile preparation of Pt–Ru nanoparticles supported on polyaniline modified fullerene [60] for methanol oxidation. *Journal of Nanoparticle Research* 2013; **15**:2061(1)–2061(7).
112. Reddy ALM, Rajalakshmi N, Ramaprabhu S. Cobalt–polypyrrole–multiwalled carbon nanotube catalysts for hydrogen and alcohol fuel cells. *Carbon* 2008; **46**:2–11.
113. Gharibi H, Kakaei K, Zhiani M, Taghiabadi MM. Effect of polyaniline-doped trifluoromethane sulfonic

acid nanofiber composite film thickness on electrode for methanol oxidation. *International Journal of Hydrogen Energy* 2011; **36**:13301–13309.
114. Zhiani M, Gharibi H, Kakaei K. Performing of novel nanostructure MEA based on polyaniline modified anode direct methanol fuel cell. *Journal of Power Sources* 2012; **210**:42–46.
115. Bashyam R, Zelenay P. A class of non-precious metal composite catalysts for fuel cells. *Nature* 2006; **443**:63–66.
116. Unni SM, Dhavale VM, Pillai VK, Kurungot S. High Pt utilization electrodes for polymer electrolyte membrane fuel cells by dispersing Pt particles formed by a precipitation method on carbon "polished" with polypyrrole. *The Journal of Physical Chemistry C* 2010; **114**:14654–14661.
117. Qu B, Xu Y-T, Lin S-J, Zheng Y-F, Dai L-Z. Fabrication of Pt nanoparticles decorated PPy-MWNTs composites and their electrocatalytic activity for methanol oxidation. *Synthetic Metals* 2010; **160**:732–742.
118. Kim Y-M, Park K-W, Choi J-H, Park I-S, Sung Y-E. A Pd-impregnated nanocomposite Nafion membrane for use in high-concentration methanol fuel in DMFC. *Electrochemistry Communications* 2003; **5**:571–574.
119. Baxter SF, Battaglia VS, White RE. Methanol fuel cell model: anode. *Journal of the Electrochemical Society* 1999; **146**:437–447.
120. Lee K, Savadogo O, Ishihara A, Mitsushima S, Kamiya N, Ota K. Methanol-tolerant oxygen reduction electrocatalysts based on Pd-3D transition metal alloys for direct methanol fuel cells. *Journal of the Electrochemical Society* 2006; **153**:A20–A24.
121. Lizcano-Valbuena WH, Paganin VA, Leite CAP, Galembeck F, Gonzalez ER. Catalysts for DMFC: relation between morphology and electrochemical performance. *Electrochimica Acta* 2003; **48**:3869–3878.
122. Gerteisen D. Transient and steady-state analysis of catalyst poisoning and mixed potential formation in direct methanol fuel cells. *Journal of Power Sources* 2010; **195**:6719–6731.
123. Bauer B, Roziere J, Jones D, Alberti G, Casciola M, Pica M. Ion conducting composite membrane materials containing an optionally modified zirconium phosphate dispersed in a polymeric matrix, method for preparation of the membrane material and its use. US Patent# 7,108,935, 2006.
124. Rajalakshmi N, Dhathathreyan KS. *Present Trends in Fuel Cell Technology Development*. Nova Science Publishers: New York, 2008.
125. Lu GQ, Wang CY. Electrochemical and flow characterization of a direct methanol fuel cell. *Journal of Power Sources* 2004; **134**:33–40.
126. Silva VS, Weisshaar S, Reissner R, Ruffmann B, Vetter S, Mendes A, Madeira LM, Nunes S. Performance and efficiency of a DMFC using non-fluorinated composite membranes operating at low/medium temperatures. *Journal of Power Sources* 2005; **145**:485–494.
127. Selahattin C, Mat MD. Measurement and estimation of species distribution in a direct methanol fuel cell. *International Journal of Hydrogen Energy* 2010; **35**:2151–2159.
128. Heinzel A, Barragán VM. A review of the state-of-the-art of the methanol crossover in direct methanol fuel cells. *Journal of Power Sources* 1999; **84**:70–74.
129. Yang H, Zhao TS, Ye Q. Pressure drop behavior in the anode flow field of liquid feed direct methanol fuel cells. *Journal of Power Sources* 2005; **142**:117–124.
130. Ren X, Springer TE, Gottesfeld S. Water and methanol uptakes in Nafion membranes and membrane effects on direct methanol cell performance. *Journal of the Electrochemical Society* 2000; **147**:92–98.
131. Kordesch K, Hacker V, Bachhiesl U. Direct methanol–air fuel cells with membranes plus circulating electrolyte. *Journal of Power Sources* 2001; **96**:200–203.
132. Gurau B, Smotkin ES. Methanol crossover in direct methanol fuel cells: a link between power and energy density. *Journal of Power Sources* 2002; **112**:339–352.
133. Zhang J, Wang Y. Modeling the effects of methanol crossover on the DMFC. *Fuel Cells* 2004; **4**:90–95.
134. Eccarius S, Garcia BL, Hebling C, Weidner JW. Experimental validation of a methanol crossover model in DMFC applications. *Journal of Power Sources* 2008; **179**:723–733.
135. Casalegno A, Marchesi R. DMFC performance and methanol cross-over: experimental analysis and model validation. *Journal of Power Sources* 2008; **185**:318–330.
136. Wang ZH, Wang CY. Mathematical modeling of liquid-feed direct methanol fuel cells. *Journal of the Electrochemical Society* 2003; **150**:A508–A519.
137. Garcìa BL, Sethuraman VA, Weidner JW, White RE, Dougal R. Mathematical model of a direct methanol fuel cell. *Journal of Fuel Cell Science and Technology* 2004; **1**:43–48.
138. Liu W, Wang C-Y. Three-dimensional simulations of liquid feed direct methanol fuel cells. *Journal of the Electrochemical Society* 2007; **154**:B352–B361.
139. Liu W, Wang C-Y. Modeling water transport in liquid feed direct methanol fuel cells. *Journal of Power Sources* 2007; **164**:189–195.

140. Seo SH, Lee CS. Impedance characteristics of the direct methanol fuel cell under various operating conditions. *Energy and Fuels* 2008; **22**:1204–1211.
141. Scott K, Taama W, Cruickshank J. Performance and modelling of a direct methanol solid polymer electrolyte fuel cell. *Journal of Power Sources* 1997; **65**:159–171.
142. Silva VSF, Silva VB, Reissner R, Vetter S, Mendes A, Madeira LM, Nunes SP. Non-fluorinated membranes thickness effect on the DMFC performance. *Separation Science and Technology* 2008; **43**:1917–1932.
143. Meyers JP, Newman J. Simulation of the direct methanol fuel cell III. Design and optimization. *Journal of the Electrochemical Society* 2002; **149**:A729–A735.
144. Meyers JP, Newman J. Simulation of the direct methanol fuel cell II. Modeling and data analysis of transport and kinetic phenomena. *Journal of the Electrochemical Society* 2002; **149**:A718–A728.
145. Kang K, Lee G, Gwak G, Choi Y, Ju H. Development of an advanced MEA to use high-concentration methanol fuel in a direct methanol fuel cell system. *International Journal of Hydrogen Energy* 2012; **37**:6285–6291.
146. Park Y-C, Kim D-H, Lim S, Kim S-K, Peck D-H, Jung D-H. Design of a MEA with multi-layer electrodes for high concentration methanol DMFCs. *International Journal of Hydrogen Energy* 2012; **37**:4717–4727.
147. Lufrano F, Baglio V, Blasi OD, Staiti P, Antonucci V, Aricò AS. Design of efficient methanol impermeable membranes for fuel cell application. *Physical Chemistry Chemical Physics* 2012; **14**:2718–2726.
148. Xu C, Zhao TS, He YL. Effect of cathode gas diffusion layer on water transport and cell performance in direct methanol fuel cells. *Journal of Power Sources* 2007; **171**:268–274.
149. Yang H, Zhao TS, Ye Q. Addition of non-reacting gases to the anode flow field of DMFCs leading to improved performance. *Electrochemistry Communications* 2004; **6**:1098–1103.
150. Danilov VA, Lim J, Moon II, Chang H. Three-dimensional, two-phase, CFD model for the design of a direct methanol fuel cell. *Journal of Power Sources* 2006; **162**:992–1002.
151. Argyropoulos P, Scott K, Taama WM. Gas evolution and power performance in direct methanol fuel cells. *Journal of Applied Electrochemistry* 1999; **29**:661–669.
152. Yang Y, Liang YC. Modelling and analysis of a direct methanol fuel cell with under-rib mass transport and two-phase flow at the anode. *Journal of Power Sources* 2009; **194**:712–729.
153. Rice J, Faghri A. A transient, multi-phase and multi-component model of a new passive DMFC. *International Journal of Heat and Mass Transfer* 2006; **49**:4804–4820.
154. Yang H, Zhao TS. Effect of anode flow field design on the performance of liquid feed direct methanol fuel cells. *Electrochimica Acta* 2005; **50**:3243–3252.
155. Argyropoulos P, Scott K, Taama WM. Carbon dioxide evolution patterns in direct methanol fuel cells. *Electrochimica Acta* 1999; **44**:3575–3584.
156. Seo SH, Lee CS. Effect of operating parameters on the direct methanol fuel cell using air or oxygen as an oxidant gas. *Energy and Fuels* 2008; **22**:1212–1219.
157. Yuan Z, Zhang Y, Li Z, Zhao Y, Liu X. Investigation of mass transport and cell performance on μDMFC with different anode flow fields. *International Journal of Energy Research* 2013. doi:10.1002/er.3013.
158. Hsieh S-S, Wu H-C, Her B-S. A novel design for a flow field configuration, of a direct methanol fuel cell. *Journal of Power Sources* 2010; **195**:3224–3230.
159. Seo SH, Lee CS. A study on the overall efficiency of direct methanol fuel cell by methanol crossover current. *Applied Energy* 2010; **87**:2597–2604.
160. Silva VS, Schirmer J, Reissner R, Ruffmann B, Silva H, Mendes A, Madeira LM, Nunes SP. Proton electrolyte membrane properties and direct methanol fuel cell performance II. Fuel cell performance and membrane properties effects. *Journal of Power Sources* 2005; **140**:41–49.
161. Jung G-B, Su A, Tu C-H, Weng F-B. Effect of operating parameters on the DMFC performance. *Journal of Fuel Cell Science and Technology* 2005; **2**:81–85.
162. Aricò AS, Cretì P, Antonucci PL, Cho J, Kim H, Antonucci V. Optimization of operating parameters of a direct methanol fuel cell and physico-chemical investigation of catalyst–electrolyte interface. *Electrochimica Acta* 1998; **43**:3719–3729.
163. Scott K, Taama WM, Argyropoulos P, Sundmacher K. The impact of mass transport and methanol crossover on the direct methanol fuel cell. *Journal of Power Sources* 1999; **83**:204–216.
164. Krewer U, Yoon H-K, Kim H-T. Basic model for membrane electrode assembly design for direct methanol fuel cells. *Journal of Power Sources* 2008; **175**:760–772.
165. Dutta K, Kumar P, Das S, Kundu PP. Utilization of conducting polymers in fabricating polymer electrolyte membranes for application in direct methanol fuel cells. *Polymer Reviews* 2014; **54**:1–32.
166. Dutta K, Das S, Kumar P, Kundu PP. Polymer electrolyte membrane with high selectivity ratio for direct methanol fuel cells: A preliminary study based on blends of partially sulfonated polymers polyaniline and PVdF-co-HFP. *Applied Energy* 2014; **118**:183–191.